

Received November 23, 2021, accepted December 2, 2021, date of publication December 8, 2021,
date of current version December 21, 2021.

Digital Object Identifier 10.1109/ACCESS.2021.3134170

Adaptive Clip Limit Tile Size Histogram Equalization for Non-Homogenized Intensity Images

ALI FAWZI^{ID1,2}, ANUSHA ACHUTHAN^{ID1}, (Member, IEEE), AND BAHARI BELATON^{ID1}

¹School of Computer Sciences, Universiti Sains Malaysia, Penang 11800, Malaysia

²Department of Computer Sciences, College of Science, University of Baghdad, Baghdad 10071, Iraq

Corresponding author: Anusha Achuthan (anusha@usm.my)

This research was funded by the Ministry of Higher Education Malaysia for the Fundamental Research Grant Scheme with Project Code: FRGS/1/2019/ICT02/USM/03/1.

ABSTRACT Intensity inhomogeneity, hidden details, poor image contrast due to low capturing device quality, limited user experience, and inappropriate environment setting during data acquisition are major issues reported during the image enhancement process. Histogram Equalization (HE) approaches have been commonly deployed to overcome the above-listed problems, apart from improving image contrast. Nevertheless, the resulting images retrieved after undergoing these approaches are often affected by undesired artifacts, unnatural looks, and unpleasant washed-out effects. As such, this study introduces a new approach called Adaptive Clip Limit Tile Size Histogram Equalization (ACLTSHE). The ACLTSHE initially assigns the optimum clip limit (CL) and tile size minimum or maximum values. Then, a new fitness function called DataSignal is deployed to produce a set of non-dominated solutions by adaptively computing the optimum CL value. The performance of the proposed ACLTSHE approach was assessed and compared with conventional Clip Limit HE (CLHE) and several state-of-the-art approaches, such as Dynamic Clipped HE (DCLHE), Iterated Adaptive Entropy Clip Limit HE (IAECHE), Mean and Variance Sub-image HE (MVSIEHE), and Adaptive Entropy Index HE (AEIHE). The outcomes were assessed both qualitatively and quantitatively by using six evaluation metrics, Discrete Entropy (DE), Absolute Mean Brightness Error (AMBE), Peak Signal-to-Noise Ratio (PSNR), Contrast Improvement Index (CII), Root Mean Square Error (RMSE), Structure Similarity Index (SSI) and Standard Deviation (SD). The quantitative evaluation of three dataset images (Pasadena-houses 2000, faces 1999, and BraTS 2019) verified that the proposed approach outperformed the compared approaches in terms of improved DE, enhanced contrast, and highlighted local details without losing the original image structures.

INDEX TERMS Histogram equalization-based technique, histogram entropy, histogram clip limit, tile size.

I. INTRODUCTION

To date, numerous acquisition image devices are at avail, such as medical scanners, digital cameras, drones, and security cameras. Some of the most common deficiencies related to the process of image acquisition are poor contrast, intensity inhomogeneity, hidden or overlapping small edges details, noise, and blur effects. Small or hidden details in images refer

The associate editor coordinating the review of this manuscript and approving it for publication was Felix Albu^{ID}.

to objects or structures that represent important information but are unclear to human eyes due to poor contrast or insufficient image brightness. These degenerations in the quality of images stem from non-uniform distribution of image intensity and inadequate lighting conditions, structural complexity of tissues and organs (e.g., common in medical images), and inappropriate camera settings. Images produced in such an environment display a restricted range of gray-level distribution and lower intensity frequencies, leading to intensity inhomogeneity, low contrast, and low-quality images [1].

Non-uniform gray-level distribution and low contrast may degrade the performance of subsequent image processing, such as image segmentation [2]. Enhancing image intensity boosts information richness in images, particularly in terms of edges, information, contrast, and regions boundaries, which facilitate human visual perception and computerized image analysis [3]. Increasing information richness of images, resulting in a homogeneous distribution of contrast across the full spectrum of image intensities, is good, practical, and widely applied in emerging applications, such as medical imaging, facial recognition, satellite image analysis, and certain military applications [4]. Information richness is achieved by correcting the pixel intensity distribution, as well as by widening the gap between the object(s) of interest and their context in the resultant images [5], [6]. The two approaches that improve the information richness of images are frequency and spatial domains [5]. The first approach enhances an image by transferring it into the frequency domain in three steps: (i) computes the Fourier image transformation, (ii) multiplies the results using a filter transfer function, and (iii) performs reverse Fourier image transform to obtain the resultant enhanced images. Fourier image transformations are performed by deploying discrete cosine transforms or discrete wavelet transforms [6]. The benefits of frequency domain-based image enhancement lie in its ability to control the compositions of the image frequency. Some drawbacks of this approach are (i) its failure to concurrently improve all regions of the entire image and (ii) the complexity of automating the procedure for image enhancement that depends totally on user experience [1]. The second approach refers to spatial domain that directly manipulates the pixel values of an image [7]. In spatial domain, different state-of-the-art approaches are proposed to increase information richness of images, including Histogram Equalization, grouping of gray levels, and unsharp masking [8].

This present study introduces a new variant of the HE-based contrast enhancement approach for correction unhomogenized intensity images, namely Adaptive Clip Limit Tile Size Histogram Equalization (ACLTSHE). This proposed method aims to increase information signals and highlight the important details of the original image while maintaining its original structure. This approach assures uniform intensity distribution across the enhanced images by setting the enhancement parameters automatically and adaptively. The proposed approach addresses the subjective issue of users while enhancing the local image details by neither generating undesired artifacts nor amplifying noise.

The next section discusses the literature review of typical HE-based contrast enhancement approaches and the respective challenges. The methodology used to design the ACLTSHE approach is described in Section III. Section IV elaborates the data sample and the benchmark metrics functions used to assess the performance of ACLTSHE. Section V presents the resultant image and performance comparison. Finally, Section VI concludes this paper.

II. LITERATURE REVIEW

The key idea of conventional histogram equalization (CHE) is to redistribute image intensity to a new uniform distribution and enhance image quality. In order to improve the overall contrast of an image, CHE modifies the cumulative density function (CDF) to redistribute the intensity of gray levels of images [9]. Uniform intensity distribution is attained when the gray levels with lower-intensity recurrence merge while increasing the disparity between gray levels with high-intensity recurrence. Essentially, HE improves the contrast of the entire image and makes the image enhancement approach simple and reliable [10]. Due to its simplicity, efficacy, and low computation time, this category has been widely applied in modern applications [4]. Nevertheless, this approach suffers from washed-out and distortion effects in the resultant images; this is back to alter the mean values of the original image [11]. When more gray levels have high frequencies, the resultant images display non-homogenized intensity distribution in the background and in other small sections.

Furthermore, this approach cannot maintain the information of the original images. These shortcomings cause contrast stretching at particular gray levels and loss of small details at lower gray levels [12]. The four CHE-derived groups are Region Histogram Equalization (RHE), Image Division, Modified Histogram Equalization (MHE), and Metaheuristic based Histogram Equalization.

A. REGION HISTOGRAM EQUALIZATION (RHE)

The RHE is the first-class derived from HE that splits the histogram into regions. This approach improves image brightness based on formulated regions and produces realistic images (non-under or over-enhanced), such as the global histograms category. Some approaches are purposely designed under this sub-class to preserve image brightness in non-homogenous intensity images, such as exposure-based sub-image HE (ESIHE) [7], Exposure Region-based Multi-HE (ERMHE) [13], Median and Mean Bi-HE plateau limit (Mean-BHEPL & Median-BHEPL) [14], adaptive Bi-HE (ABHE) algorithm [14], and Nonlinear Exposure Intensity-Based Modified HE (NEIMHE) [15]. By applying the exposure threshold, the ESIHE approach splits the image's histogram into two areas, and both sub-histograms will be clipped using the gray level's mean value. Then CHE can also be applied for sub-histograms.

The ESIHE method offers good preservation of local details and contrast enhancement but does not perform properly with samples containing multi-exposure areas (i.e., normal, under-, and - overexposure). Both ABHE and BHEPL approaches are proposed to overcome the limitation of ESIHE by working with overexposure and underexposure exposure regions. However, they do not perform well with images that have normal exposure areas. The ERMHE approach tackles the problem of multi-exposure regions. Although the approach offers good quality of brightness and

lower noise in resulting images, one exposure area can be greater than the other(s). This issue can cause the problem of dominant high frequency over frequencies of lower intensity, thus loss of information in some parts.

A more recent study by [15] showed that a Nonlinear Exposure Intensity-Based Modified HE (NEIMHE) enhanced non-uniform illumination images. The NEIMHE approach splits the input image into five sub-regions and transforms the histogram of each sub-region by assigning a nonlinear weight to its cumulative density function (CDF). The stretching of intensity and different directions of intensity mapping for normal, over-exposure, and under-exposure sub-regions are provided by the modified HE equations, which are later used to equalize each modified histogram. The NEIMHE used fixed grey level ranges for intensity mapping determined according to the well-exposed region, perhaps leading to under-or over-enhancement issues.

B. IMAGE DIVISION

Image division is the second sub-class derived from CHE. The image division was developed approaches to address the limitations of HE by modifying and improving the information richness of non-overlapping contextual gray-level regions derived from the image while retaining information by filtering through all image pixels. The division in this sub-class is classified by pixels and histogram-based divisions. The pixels division relies on cutting the image into small tiles. For example, an image with 100×100 pixels can be divided into ten tiles. The size of each tile is 10×10 pixels. The division of histogram depends on a specific value computed from the histogram of the image to divide it into sub-histograms.

1) PIXELS-BASED DIVISION

Pixels-based division techniques improve small gray-level regions and retain image details by mapping the limited scope of pixels of an image to the entire visualization range. It is designed to address the low contrast issue in the HE class by splitting the input image histogram into multiple tiles. Some approaches proposed in this category include Adaptive Histogram Equalization (AHE) [16], Partially Over-loaded Sub imaging HE (POSHE) [17], Contrast-Limited Adaptive HE (CLAHE) [18], Adaptive image enhancement method based on Multiple Layers Quick Block Overlapped HE (BOHE) [19], and Multidimensional CLAHE (MCLAHE) [20].

The AHE approach determines a block of pixels (e.g., 6×6) and maps its center in a horizontal or vertical orientation from pixel to pixel. For each exposure, the histogram of the points in the neighborhood is calculated and equalized. The intensity of the pixel lying in the center of the region is measured. Next, the position center point of the region is shifted to a neighboring pixel, and this task is iterated [21]. For instance, an image with 640×480 dimensions must be manipulated 307,200 times by the histogram process to yield the resultant image. The AHE

approach addresses the intensity inhomogeneity drawback of HE by operating on wholly image pixels to produce resultant images with uniform intensity distribution. But, AHE amplifies the noise in the result images and consumes the longest running time [17]. The approaches of CLAHE and POSHE also suffer from unnatural appearance in the resultant images [16]. In some cases, CLAHE and POSHE generate images with noise effects and poor appearance [22]. In computing time, POSHE has shown limited progress [17].

In order to enrich local details and decrease the noise effect of the resultant images, multiple enhancement stages were proposed in [19]. The approach applies the Quick Block Overlapped HE (BOHE) approach to various tile sizes produced from the original input image in multi-layer enhancement. Next, the CLAHE approach decreases the noise of each tile. The result of the last step is split into smaller components then fused to produce the resultant image with retaining the local details. This approach is subject to some drawbacks, including intensity non-homogeneity, long-running time, inability to enhance the brightness of the resultant images, and failure to maintain the original edge information of the input image in the resultant image.

Furthermore, [20] designed and employed Multidimensional CLAHE (MCLAHE) to enhance spectroscopic and fluorescence microscopy datasets with arbitrary dimensions. This method uses data padding to produce an image with a random number of dimensions using the Lagrange form of multilinear interpolation. Finally, an adaptive histogram range is introduced to improve the spatial adaptivity of the conventional CLAHE approach to the intensity domain to reduce the effects of artifacts. However, the model suffers from two drawbacks: (i) high computation and memory complexity, (ii) the approach is sensitive to parameters and can only produce high image quality upon careful parameter setting.

2) HISTOGRAM-BASED DIVISION

This approach is used to preserve image intensities by dividing the original image histogram into sub-histograms. The two sub-categories of this approach can be classified into dual and multiple sub-histograms. Approaches that derive from the dual sub-histogram category are Dual Sub-Image HE (DSIHE) [23], Brightness Preserving HE (BBHE) [11], and Minimal Mean Brightness Error Bi-HE (MMBEBHE) [24]. Entropy-based BBHE (EBBHE) [25], Otsu-based BBHE (OBHBE) [25], and Range-Limited Bi-HE (RLBHE) [26] are also proposed.

The MMBEBHE method searches for a threshold value that maintains the minimum value for brightness error. The approach of DSIHE focuses on the histogram median value, while BBHE depends on the histogram mean value. However, these approaches suffer from a high-frequency dominance issue if many dominant gray levels are present in the sub-histogram. HE alike, these approaches may produce an enhanced image with a high degree of noise that cannot retain image details and (ii) long computation time [27].

Both EBBHE and OBBHE use entropy and Otsu based on the image histogram threshold. These approaches preserve image brightness, and the resultant images are the best in terms of information richness compared with images yielded from BBHE, DSIHE, and MMBEBHE approaches. Nevertheless, the resultant images by these techniques suffer from poor enhancement in image contrast [28].

Meanwhile, RLBHE [26] separates the image into background and foreground by splitting the histogram of the original image into two sub-histograms while preserving image brightness. Nevertheless, the produced images suffer from washed-out details.

The Dynamic Clipped HE (DCLHE) approach for improving low contrasted images [29] is another method used in the histogram-based division category. This approach enhances images by (i) eliminating all gray levels with zero frequency from the image histogram, (ii) clipping the residual gray level with non-zero frequency using the lowest histogram value, and (iii) using CHE for contrast enhancement. The approach enhances the entropy of the image and attains homogenized distribution of intensity. The drawbacks of this approach are the inability to preserve brightness and operate effectively only for a limited number of gray levels.

A new Fuzzy-based Bi-HE (FBHE) approach is proposed in [30] for optimal equalization of low-contrast images. The FBHE approach uses a level-snip technique to select the optimal threshold value for histogram partitioning. Like other bi-HE approaches, the segmented sub-histograms are equalized separately and then concatenated. Despite its effectiveness, the approach suffers from computational complexity in setting the optimum value of parameters for computing the threshold value.

The approach based on Global and Local histogram equalization and Dual Multiscale image Fusion (GLHDF) is proposed in [31] for underwater image enhancement. The GLHDF approach comprises four main stages, i.e., (i) center regionalization based on pixel intensity is performed to smooth the image and increase the similarity of the tricolor histogram. (ii) global equalization of the histogram is performed to correct the image's color based on the characteristics of RGB channels. (iii) dual-interval histogram equalization based on optimal threshold value extracted using the average of peak and mean values technique. Finally, (iv) a multiscale fusion combines the contrast improved image with the color corrected image to produce a high-quality resultant image.

Multiple sub-histogram-based image division is another category proposed for splitting the input image's histogram into multiple sub-histograms to enhance small non-overlapping contextual regions and preserve image details by manipulating the whole pixels of images. It also overcomes the limitations of the low contrast issue in the CHE class by splitting the input image's histogram into multiple sub-histograms. Some approaches proposed within this category are Recursive Sub-image HE (RSIHE) [32], Recursive Mean Separate HE (RMSHE) [33], Adaptive Thresholding-based

Sub-HE (ATSHE) [34], and Median-Mean Sub-image based Clipped HE (MMSICHE) [35].

RSIHE, RMSHE, ATSHE, and MMSICHE approaches are updated versions of the BBHE, and DSIHE approaches. The RSIHE and RMSHE select median and mean values, respectively, as the threshold of separation in a recursive manner. Due to the multiple decomposition procedure, both approaches improve brightness preservation. However, the recursive decomposition procedure results in noise amplification and lengthy computation time. Besides, the need to select the recursive level manually is subjected to human decisions, and the high value of the recursive level results in negligible image improvement [36].

The MMSICHE approach splits the histogram of the input image into four sub-histograms by setting two values to recursive levels by using the mean feature of BBHE. Next, for each sub-histogram, the median value is calculated and clipped in the same manner as DSIHE. After that, CHE is performed for the sub-histograms. The advantages of MMSICHE are (i) regulating the over contrast and (ii) improving the brightness of the image.

In order to identify the number of sub-histograms precisely at each level, ATSHE utilizes PSNR. Then, it uses mean and standard deviation values to obtain the threshold. Therefore, a multi-level distribution of histograms takes place. Next, to improve image contrast, the ATSHE method utilizes the median value for histogram clipping. This method maintains the brightness of the image with poor illumination. However, ATSHE suffers from these drawbacks: (i) manual determination of iterations number consumes long computation time that leads to negligible image enhancement, (ii) certain sections of the resultant image are washed-out and results in loss of local small edge details in the resultant image, and (iii) only a limited number of images is used to test the approach.

To ensure no intensity compression (prevent a wide range of input gray from being mapped to a limited range of output gray), having over enhancement or washed-out, Dynamic Histogram Equalization (DHE) [37] and Brightness Preservation DHE (BPDHE) [9] were proposed.

The DHE approach separates the image histogram into many sub-histograms depending on the local minimum until no dominant gray level is found in the generated sub-histograms. However, the resultant images produced by this approach are subjected to over brightness error despite comprehensively preserving the image details.

On the other hand, histogram separated using the BPDHE approach is based on local maxima and Gaussian filter. This approach addresses the issue of over-contrast in DHE. Although the approach produces varied ranges of newly sub-histograms, i.e., some newly generated sub-histograms have limited ranges of gray-level, and other gray levels have wide ranges of gray-level. Varying histogram ranges contribute to non-homogenized image enhancement [9].

Quadrants Dynamic HE (QDHE) [38] limits contrast over enhancement and noise amplification. This approach utilizes

the median value as the DSIHE approach to split the input image's histogram into four sub-histograms. For each newly generated sub-histogram, the mean value is determined to assign a threshold value to perform the clipping process. Eventually, the clipped sub-histogram yields a new dynamic range using the DHE feature.

The QDHE approach produces an image that preserves a high degree of image details. Adaptive Increases the Values of HE (AIVHE) [39] prevents serious adjustment in Probability Density Function (PDF) through redistributing the original PDF. However, determining the parameters for AIVHE is subjected to human intervention.

Moving on, to address the shortcomings of the RMSHE approach, Entropy Dynamic Sub-HE (EDSHE) [40] is developed by calculating the entropy for each recursive layer and contrasting it with the original set value. Nevertheless, the EDSHE generates unwanted artifacts in the resulting images and the processing time is lengthier than that for CHE and RMSHE methods.

The Iterated Adaptive Entropy Clip Limit HE (IAECHE) separates an image into multiple sub-images and uses an image histogram to determine the clip limit (CL) value by identifying the peaks from these sub-images [41]. The IAECHE calculates the best CL value in an iterative and adaptive process. Next, the enhanced sub-images are combined to generate the resultant image. The two drawbacks in IAECHE are: (i) no guarantee to produce the best CL values and (ii) long processing time.

In a recent study, a Three Adaptive Sub-HE (TASHE) approach was proposed by [42] for maritime image enhancement. The TASHE approach separates the input image histogram into three adaptive sub-histograms according to the characteristics of Gaussian distribution. The separated sub histogram will then be enhanced using two optimal thresholds derived adaptively from the image's histogram. The proposed TASHE approach maintains the original image's mean brightness; however, the technique is limited to be applied for the maritime images and may fail to enhance images that do not obey the Gaussian distribution.

C. MODIFIED HISTOGRAM EQUALIZATION

The approaches under the MHE sub-class control the enhancement rate of the high-frequency gray levels by modifying the image histogram. These approaches maintain the image details through clipping and transforming the histogram, thus prohibiting the bias toward dominant histogram levels. After the adjustment stage, the high-frequency histogram levels have lower impacts than the initial histogram. This causes minimal enhancement in the output image when compared to the prior approaches developed under this category, such as Modified Histogram Equalization (MHE) [12] Weighted Threshold HE (WTHE) [43], Edge Preservation Local HE (EPLHE) [44], Recursively Separated and Weighted HE (RSWHE) for contrast enhancement and brightness preservation [45], Logarithmic Law based HE scheme (LMHE) [46] to enhance natural images,

Bi-Histogram Modification (BHM) for low-contrasted and non-homogenized intensity images [47], Range Limited Weighted HE (RLWHE) [6], and Mean and Variance based image enhancement via sub-image HE (MVSIEH) [27].

The MHE was introduced to eliminate undesired artifact that appears in the resultant images generated using RMSHE, BBHE, and DSIHE approaches, consequently providing a better appearance to the resultant image. In the MHE method, the histogram of the input image is modified and then uses CHE for the enhancement task. The MHE suffers from drawbacks as follows: (i) determining the optimal parameter value that gives a reasonable improvement outcome is difficult and highly subjected to human experiences, and (ii) lowering the dominant histogram levels may result in eliminating some image information.

The WTHE adjusts the PDF values to be weighted, and then CHE is applied to the adjusted PDF to avoid the over-contrast enhancement issue adaptively. This approach is quick, but it does not keep the brightness of an image, and some unwanted artifacts are produced in the resultant image.

The approach of RSWHE is classified into RSWHE-M and RSWHE-D. While RSWHE-M calculates the mean value to split the histogram as RMSHE but in a recursive manner, RSWHE-D calculates the median value to split the histograms as RSIHE but in a recursive manner. Next, these newly generated sub-histograms are altered using the normalized power-law distribution function. After that, CHE is used for all sub-histograms, which changes the sub-histograms with the standard power-law distribution function. Both RSWHE-M and RSWHE-D provide contrast enhancement and remarkable brightness preservation, but they yield unwanted artifacts in the resultant image due to eliminating some image details [40].

The RLWHE method was proposed to control over enhancement, improve contrast, and preserve the brightness of images. This method uses the Otsu threshold to split the histogram of the input image into two sub-histograms to reduce intra-class variance. The PDF is then altered and weighted for every sub-histogram, which later uses the CHE to restrict the brightness of each sub-histogram. In the next step, adaptive gamma correction is introduced to enhance the image entropy and avoid the introduction of unwanted artifacts. Finally, a homographic filter was proposed to reduce the effects of artifacts.

The EPLHE approach claimed that when the sub-image is a part of zero-textured regions, the POSHE could not maintain the edges of the image regions [44]. Then the region's information richness would be minor, and the resultant CDF values would show insufficient changes, perhaps leading to under-or over-enhancement issues. The EPLHE method divides the image into equal size non-overlapped sub-images; then, the SOBEL operator is applied to these sub-images for detecting the edges of objects. The downside of EPLHE is that the sub-imaging procedure relies on the scale of the input image. The approach suffers from over-preservation

of brightness in dark regions, thus failing to preserve image details. It also has insufficient criteria for quantitative measurement.

The LMHE approach is proposed in two stages to maintain the natural appearance of an image. The first stage of the histogram adjustment is to use addition-based to solve the histogram pits issue [46]. In the second step, the logarithmic law-based scheme is used to solve the histogram spikes issue. Next, HE is employed to achieve global improvement, where local fine-tuning is executed using DCT on the image. However, this approach cannot maintain image brightness, thus causing dark regions in the image [47]. Nonetheless, this approach works in three steps. The suggested method considers the low-frequency gray level indicating the illumination in the first step. The Gaussian low-pass filter is applied to the image to extract illumination and to prohibit noise amplification. After that, the images are separated into dark and bright zones by computing the threshold based on the median value to retain the maximum segmentation entropy. Secondly, the histogram of the two segmented zones is shifted by moving the dark zone towards the threshold to maximize contrast. The bright zone is moved towards the highest value between median and mean to avoid the output image from appearing unnatural. In the last step, for improvement, the histogram in each zone is redistributed based on the transformation feature. This method can retain image details, decrease noise, and improve image entropy. The drawbacks of this method are: (i) some blurred parts in the output image that cannot operate with several zones, such as gray, dark, and bright zones, and (ii) the resultant image produced some artifacts.

Meanwhile, the Mean and Variance based Sub image HE (MVSIE) approach [27] splits the image histogram into four parts by considering the mean and variance in computing three adaptive thresholds. Afterward, for each section, the CHE is used for modification and equalization. Finally, the improved four sections are merged to decrease the saturation of intensity and interference via normalization. This approach maintains the image brightness and yields images without artifacts. The shortcomings of this method are (i) time consuming and (ii) inability to highlight hidden details.

D. METAHEURISTIC-BASED HISTOGRAM EQUALIZATION

The combination of metaheuristic optimization algorithms and HE-based approaches is the fifth sub-class of the HE-based image enhancement approaches. The main source of metaheuristic approaches is inspired by nature, which has motivated researchers to solve different image processing problems such as optimization, enhancement, segmentation, and classification. The nature-inspired metaheuristic approaches have been efficiently and successfully used to solve or mitigate the HE-based image enhancement issues such as the subjective effects of manual parameters setting and over-or under-enhancement. In this context, several nature-inspired metaheuristic approaches

have been hybridized with HE to address intensity inhomogeneity and to improve image contrast, as reported in [48]–[56], and [57].

The Particle Swarm Optimization (PSO) was hybridized with the CLAHE approach to improve mammogram images [48]. The PSO is used to increase the information richness and highlights edge information. The optimized version of parameterized bi-threshold HE was introduced by determining the entropy value in a real-coded genetic algorithm (GA) for enhancing Magnetic Resonance Images (MRI) of brain images [49]. Another study proposed the multi-objective Cuckoo Search Algorithm (CSA) to improve mammogram images by combining CSA with Otsu-Based Bi-Weighted Threshold HE (OBBWTHE) that generated a quality index based on fractal dimension and local variance [50].

The hybridized approach between Artificial Bee Colony (ABC) algorithm and Multi-threshold HE MTHE is elaborated in [51] to maximize the entropy value as the objective function for enhancing histopathology images. A new hybridization method for enhancing the medical images, a firefly algorithm with OBBWTHE, and CLAHE were introduced in [52]. The approach utilized the firefly algorithm to compute the PSNR value as an objective function.

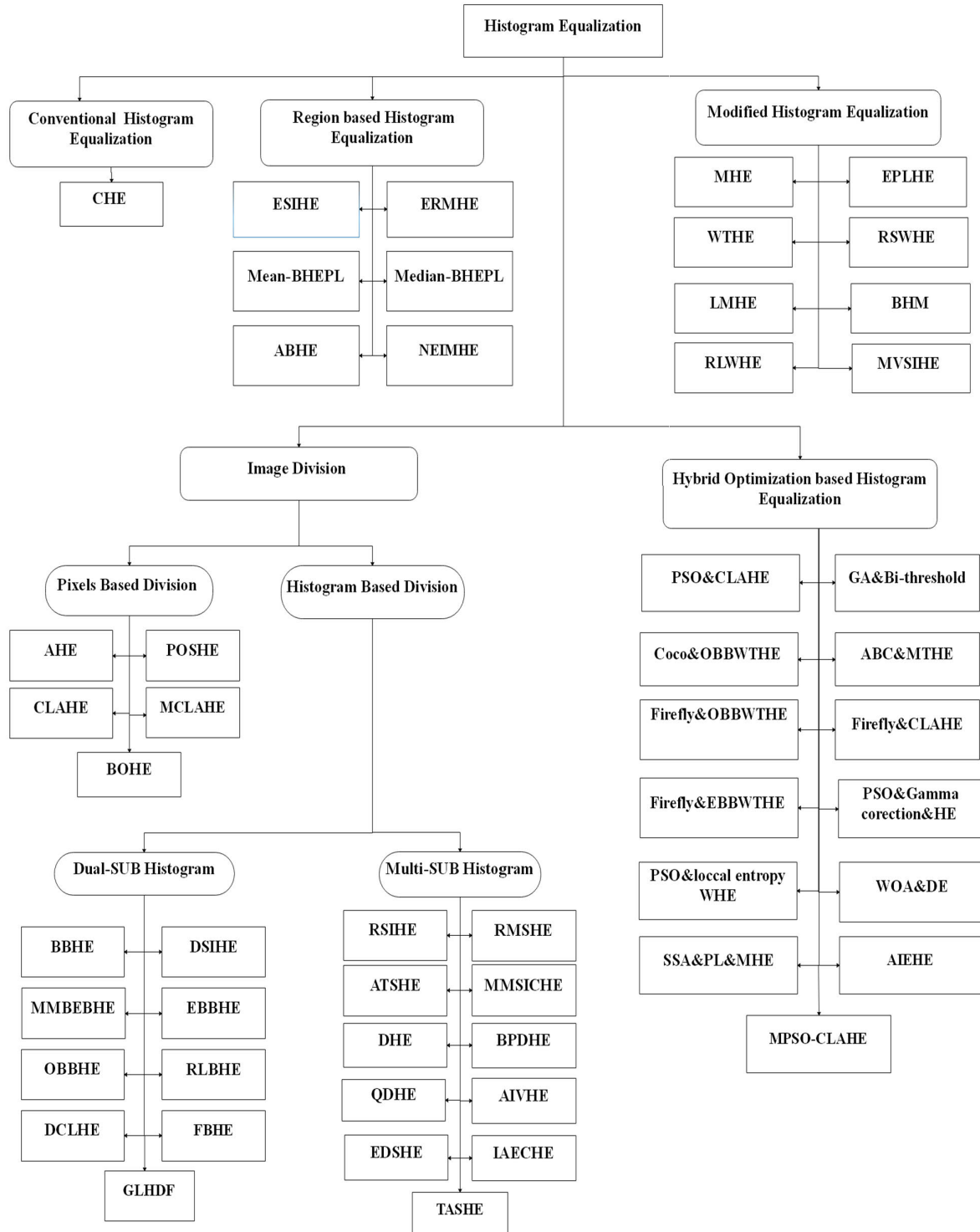
In [53], PSO was deployed to maximize the entropy value, which was later combined with gamma-correction to enhance satellite images. Another study introduced the hybridized method of PSO with local-entropy-weighted HE to maximize entropy value for infrared images in [54].

As depicted in [55], the hybridized differential evolution with the whale optimization method was devised to improve image contrast. The objective function in this approach is formulated as a hybridization of edge intensities and image entropy. However, the approach was assessed on a limited amount of images.

Another fitness function for image enhancement is proposed in [56]. The method depends on the slap folks swarm optimization method to obtain the best percentage of image entropy with PSNR of an image and edge intensities. The method yielded improved images with homogeneous intensity and preserved brightness. However, the approach consumed a long time to obtain the optimum value, and the setting of parameters was subjected to user experience.

In a recent study, the CLAHE approach combined with a whale optimization method termed AIEHE was proposed by [57] for poor contrast images enhancement. The AIEHE approach separates the input image into three sub-images. The separated sub-images will then be enhanced separately using adaptive and automatic enhancing parameters (window size and clip limit). Finally, the resultant image is produced by combining the enhanced sub-images.

A more recent study by [57] investigated an approach for enhancing retinal fundus images using the hybridized modified PSO with the CLAHE (MPSO-CLAHE) approach.

**FIGURE 1.** Histogram equalization and its sub-classes.

Firstly, the PSO is modified to overcome its drawbacks then applied for CLAHE parameter tuning (contextual region and clip limit).

In general, each category obviously has some shortcomings. The CHE group suffers from washed-out effects and loss of small local details. The image division group suffers from

TABLE 1. Summary of HE-based contrast enhancement techniques.

Category	Approach	Advantages	Drawbacks
CHE	[10]	<ul style="list-style-type: none"> • Easy • Effective • Low computation time • Homogeneous gray level distribution 	<ul style="list-style-type: none"> • Washed-out • Loss of local image details • Poor performance with dominant gray level • Over enhancement • Cannot preserve brightness
RHE	[7], [13-15]	<ul style="list-style-type: none"> • Preserve brightness • Segmentation threshold depends on exposure parameter 	<ul style="list-style-type: none"> • Poor performance on image with multiple exposures that may affect the contrast of good-exposed regions • Vast details are washed-out
Image division	[9], [11], [16-20], [23-26], [29-35], [37-42]	<ul style="list-style-type: none"> • Preserve image local details • Better enhancement for low frequency pixels • Reduce noise • Control clipping enhancement • Preserve entropy • Reduce noise 	<ul style="list-style-type: none"> • Poor performance and images have non-uniform distribution • Artifacts • Subjective parameters • Require skillful users • Long computation time • Irregular appearance
MHE	[6], [12], [27], 43-47]	<ul style="list-style-type: none"> • Better enhancement for low frequency bins • Preserve brightness • Reduce noise 	<ul style="list-style-type: none"> • Preserve details • Difficult to find optimal threshold parameter • Long computation time
Metaheuristic Based Histogram Equalization	[48-57]	<ul style="list-style-type: none"> • Dismiss prior knowledge about the problem • Automatic parameter initialization • Improve response signal-to-noise ratio 	<ul style="list-style-type: none"> • Long computational time • Parameters value • High complexity to compute the optimum fitness function • Limited local and global search

long running time and difficulty in finding the optimum level of sub-images. In dominance gray-level, the MHE category suffers from losing details, whereas the RHE approach suffers from unwanted artifacts and washed-out effects in a large span.

A descriptive diagram of the CHE and its sub-class approaches are illustrated in Figure 1, while Table 1 lists the summary of advantages and drawbacks for each category.

Three observations can be made from Table 1, as follows:

1. Each class has some drawbacks and could not simultaneously resolve all common issues in digital images.
2. Most current approaches require parameters to be set manually, thus time-consuming and subject to the knowledge and skills of users.
3. Inappropriate initialization and setting of parameters can yield poor outcomes (under- or over-enhanced image).
4. Although some approaches can improve the local image details, their drawbacks create an unnatural appearance in the output images.

Issues related to noise, non-uniform intensity, unwanted artifacts, and washed-out effects have led this study to

develop a new enhancement approach based on the image division trend.

The proposed approach aims to increase information richness, achieve uniform intensity distribution, and highlight the enhanced images' local details. The proposed approach offers a uniform distribution of intensities on the resultant images without amplifying noise or creating undesired artifacts, thus solving the non-uniform intensity issue. The proposed approach incorporates an intelligent approach to initialize and set the enhancement parameters adaptively and automatically to address the subjective issue of manual parameter setting of the enhancement process.

Seven quantitative evaluation metrics, (i) DE, (ii) PSNR, (iii) CII, (iv) AMBE, RMSE, (v) SSI, and (vi) SD, are used to assess the quality of the resultant images against other state-of-the-art approaches.

III. CONTRAST LIMITED ADAPTIVE HISTOGRAM EQUALIZATION

The CLAHE approach is a member of the Pixels-based division sub-class. It was designed specifically to improve the low-contrasted medical images [58], [59]. The CLAHE

approach divides the original input images into contextual sub-images, called blocks or tiles. The two major parameters for this approach: tile size (TS) and CL, are used to regulate the contrast of the enhanced images. The contrast degree of the output images is highly affected by the CL value so that the large CL value flattens the histogram of the output images. Meanwhile, a small TS value expands the dynamic gray level range, thus reducing image contrast.

The CLAHE approach computes the image histogram for every sub-image, and the computed histograms are clipped for each contextual region, whereby the clipped pixels are distributed at each gray level. The newly produced histograms differ from the original ones since the intensity of image pixels is limited for the wholly gray levels that are limited to the value of CL. The dimensions (width & height) of the tiles are manually set. The histogram of tile is computed, while the normalized CL is determined. The real CL is then determined from the normalized CL, which is used to evaluate the criterion for the histogram clipping of the sub-images.

The CLAHE approach calculates the number of pixels for the intensity that belongs to each sub-image, which is later equated with CL. The amount of pixels that belong to each intensity value is limited to the value of CL. The remaining pixels (above CL value) are distributed to fill the entire range of intensity levels of the sub-images. Next, a transform function is applied to the output for tuning the resultant image to display a more realistic appearance. By applying the bi-linear interpolation function to the sub-image pixels, the effect of artifacts is minimized. Finally, all enhanced sub-images are combined to reconstruct the resultant image with enhanced quality.

The CLAHE approach has several advantages over the AHE approach, such as being adaptive and decreasing noise amplification by clipping and redistributing the histogram using a predetermined value before calculating CDF. The CLAHE approach differs from the CHE approaches by dividing the input image into multiple tiles, then computing different histograms for each tile and using them to enhance the image contrast. Hence, CLAHE improves the visualization quality of the input images and results in a better entropy value for the resultant images. However, CLAHE suffers from the following shortcomings:

1. It improves the intensity of both image regions (background and foreground) by the same weight, thus producing a highly contrasting output image in both regions, which amplifies the noise in homogenous regions, and the appearance of the output image becomes unnatural.
2. It improves the intensity of both image regions (background and foreground) by the same weight, thus producing a highly contrasting output image in both regions, which amplifies the noise in homogenous regions, and the appearance of the output image becomes unnatural.
3. It takes a lengthy running time to produce an enhanced image because the input image is divided into small TS

to improve a small gray-level area and to avoid image details loss.

4. CLAHE is a subjective task and heavily relies on the user's prior knowledge to manually set the enhancement parameters (TS and CL). Setting a large CL value flattens the distribution of pixels over the histogram of gray-level and amplifies the noise while setting a small CL value could lead to bare improvement of image contrast. Various images need different CL settings. Next, the TS value influences the natural quality of the resultant images. Assigning a small TS value retains fewer local image details and avoids amplifying the noise in the resultant image. While assigning a large TS value also amplifies noises and preserves more local image details in the resultant images; thus, creating undesirable output images. Besides, setting the standard values of CLAHE parameters (TS & CL) may result in unnatural appearance and over-enhanced contrast. Therefore, selecting the optimal parameter value in the CLAHE approach is crucial for good quality enhanced images. This study introduces a new adaptive method called ACLTSHE to compute the optimum CL range and tile size automatically in order to overcome the subjective issue of manually setting the parameter value, apart from addressing over-enhancement issues and unnatural effects on the resultant images.

IV. THE PROPOSED ADAPTIVE CLIP LIMIT TILE SIZE HISTOGRAM EQUALIZATION

This study theorizes that the weight of enhancing the background region should not be equal to the weight of the foreground regions. The reason behind that is the foreground region consists of the main objects, and valuable data in the image is called a region of interest, while the background is composed of homogenous objects and less valuable data, such as sky, sea, black background of medical images, and wall. Thus, obtaining the best resultant enhanced image with highlighted local details is restricted on three factors: (i) attained higher local information richness, (ii) increased information signal, and (ii) minimized image distortion. To achieve these assumptions, the proposed ACLTSHE approach focuses on achieving the multiple objectives of obtaining the best value of DE to highlight the local details of the image, reducing the computation time, as well as to reduce the difference between input and resultant images by increasing the PSNR value and reducing the error between the input and resultant images by increasing the SSI value. These assumptions are set to control over-enhancement and subjective parameters setting issues in the conventional CLAHE, apart from generating a pleasant resultant image.

The proposed ACLTSHE approach is designed from three main stages: (A) obtaining the optimum tile size and CL range, (B) obtaining the optimum CL value, and (C) producing the resultant image. In the first stage, the proposed ACLTSHE approach seeks to obtain the optimum tile size ($Optimum_{TS}$) and the optimum CL range

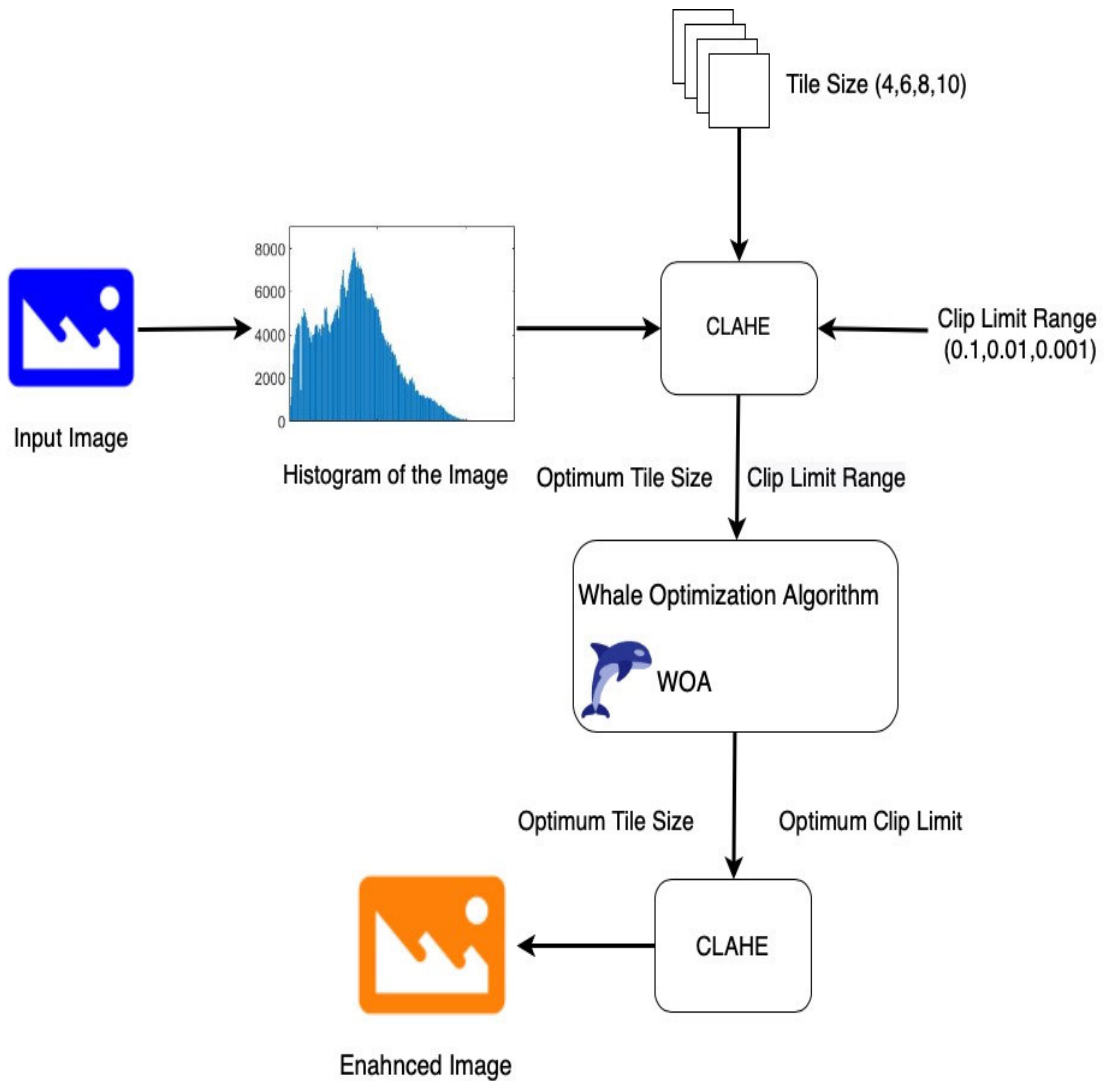


FIGURE 2. Block diagram of the ACLTSHE technique.

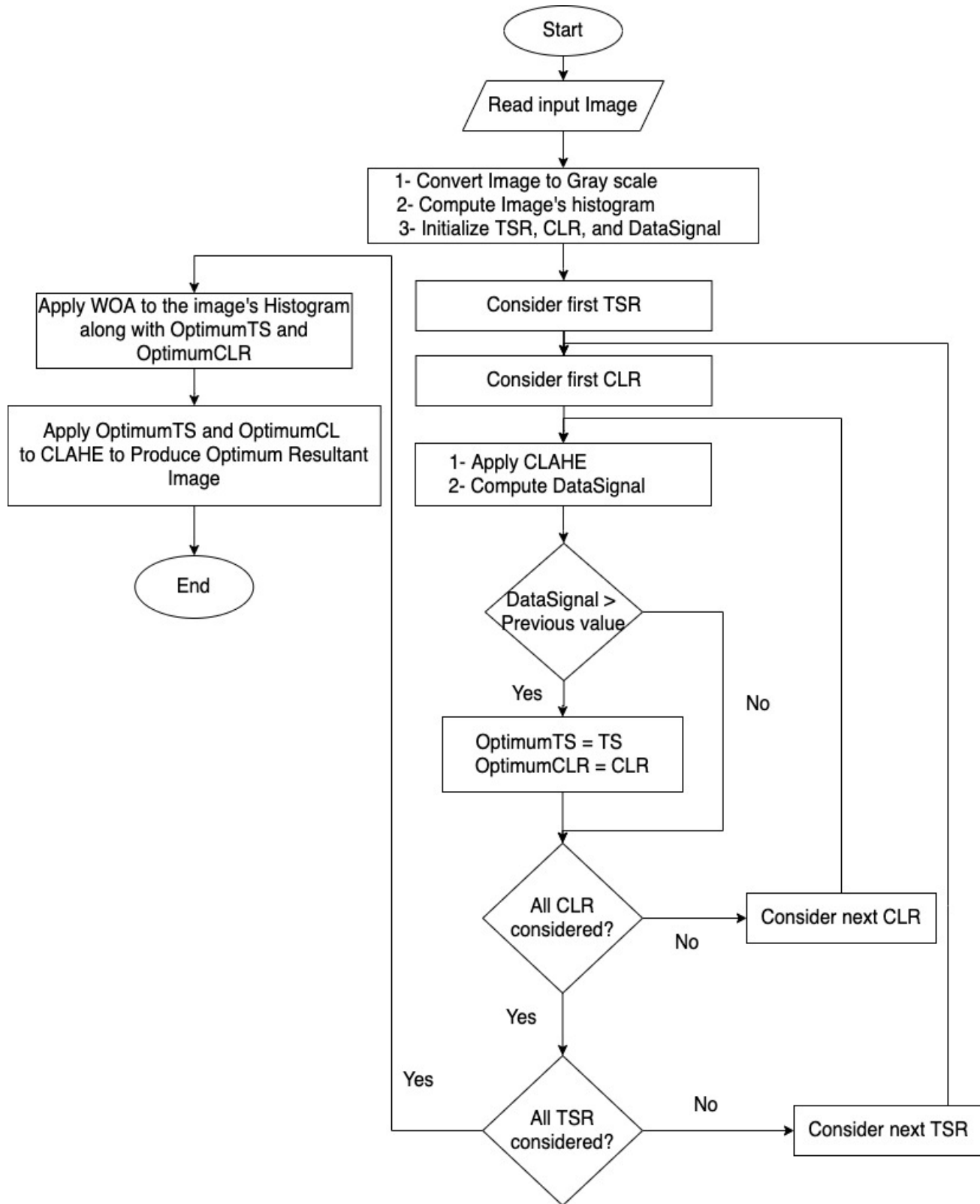
($Optimum_{CLR}$). In the second stage, the Whale Optimization Algorithm (WOA) is applied to achieve the optimum CL ($Optimum_{CL}$) value. The WOA is a metaheuristic optimization algorithm that simulates the food source chasing of the humpback whale by spreading bubbles net around the food source as a hunting strategy (refer to [57] for more details about WOA). In the final stage, two values ($Optimum_{TS}$ & $Optimum_{CL}$) are applied as input parameters to the standard CLAHE in yielding the enhanced image. Figures 2 and 3 illustrate the block diagrams of the proposed approach, the working stages, and the flowchart of the proposed approach, respectively. Sub-sections A, B, and C elaborate the working stages of the proposed ACLTSHE technique.

A. COMPUTATION OF OPTIMUM TILE SIZE AND CLIP LIMIT RANGE STAGE

The proposed ACLTSHE approach reads the input image and converts it from a color-based image to a gray level-based

image. Next, the image histogram is computed to allocate the optimum input parameters of the CLAHE approach. The proposed approach assumes that a small number of tiles (TS) (e.g., 2 & 4) and dividing the image have less priority as input parameters value to the enhancement process. This assumption is based on the idea that these small values barely enhance the image or highlight the local and hidden details. Accordingly, tile sizes ranges (TSR) of (6, 8, & 10) are applied at the first stage of the proposed approach to obtain $Optimum_{TS}$. Sizes above (10) adversely affect the enhancement process because large tile size can lead to contrast over-enhancement issue and long computation time. The value of $Optimum_{TS}$ is used in the second stage to guarantee the selection of the $Optimum_{CL}$ value from the $Optimum_{CLR}$ and in the third stage to yield the resultant enhanced image.

Based on the mentioned assumption, the three values of TSR (6, 8, & 10) were applied to the conventional CALHE, along with a vector of various CLR values (i.e., 0.1000,

**FIGURE 3.** Flowchart of the proposed technique.

0.0100, & 0.0010). The *CLR* values were set to (0.1000, 0.0100, & 0.0010), while all values smaller than this value

(e.g., 0.0001) were neglected due to (i) the low impact on the enhancement process and negligible improvement on the

TABLE 2. Minimum and Maximum CL value of each CLR.

CLR	Minimum CL	Maximum CL
0.1000	0.1000	0.9999
0.0100	0.0100	0.0999
0.0010	0.0010	0.0099

resultant image, and (i) the higher convergence speed of WOA towards the best solution by decreasing the search space. The range values for both *TSR* and *CLR* were selected for pre-experiment analysis. Table.2 lists the three values of *CLR* with maximum and minimum values of each range. If the selected value is 0.0010, then the *OptimumCL* value will be restricted between 0.0010 and 0.0099; thus, reducing the computation time in the second stage.

The benefit of this stage is obtaining *OptimumTS* and *OptimumCLR* by applying *TSR* values and all *CLR* values as input, along with the computed histogram of the image to the conventional CLAHE. Next, the new image quality factors that consisted of *DE* and *PSNR* were computed for each pair of values (i.e., a value from *TSR* and a value from *CLR*). The values of these factors were multiplied to produce a new quality factor as a multi-objective fitness function to this approach called *DataSignal*, as expressed in Equation 1:

$$\text{DataSignal} = \text{DE} \times \text{PSNR} \quad (1)$$

where *DE* and *PSNR* represent the image's information richness and the resultant tile size index, respectively, the value of *DataSignal* factor was compared with the previous value and the largest value, along with the corresponding *OptimumTS* and *OptimumCLR* values as they were used in the second stage to obtain the *OptimumCL* value. Based on the three values of *TSR* and *CLR*, only nine iterations were produced to gain only one value for *OptimumTS* and *OptimumCLR* (as tabulated in Table.3). Figure 4 illustrates the pseudo-code of the first stage.

B. COMPUTATION OF OPTIMUM CLIP LIMIT VALUE STAGE

The essential function of the second stage is to compute the *OptimumCL* value from the selected range of *OptimumCLR* allocated in the previous stage. This process depends on the fitness function of the WOA algorithm, as this algorithm relies on the natural behavior of the whale to seek food sources and feed on the valuable one. To mimic this strategy in WOA, there is a possibility of 50% to select between the spiral model and the shrinking encircling mechanism to perform both exploring and exploiting tasks, as well as updating the position of search agents during optimization tasks.

Let's assume the best values of the *TSbest* and *CLRbest* pair as (6, 0.0100). In this stage, the functionality of WOA is obtaining the best value of CL in the range of (0.0100 to 0.0999) for the TS value of 6. Consequently, the WOA

TABLE 3. The iterations of combining all tile sizes with all clip limit ranges.

Iterations	Tile size (TS)	Clip Limit Range (CLR)
1	6	
2	8	0.1000
3	10	
4	6	
5	8	0.0100
6	10	
7	6	
8	8	0.0010
9	10	

```

1: Begin
2: Read input Image
3: Convert image from colour to gray scale
4: Compute Image histogram
5: Initialize TS = {6,8,10}, CLR = {0.1000,0.0100,0.0010}, TS_Counter = 0, CLR_Counter = 0, maxDE =0, maxPSNR =0, OptimumTS =0, OptimumCLR =0
6: For 3 <- TS_Counter = 1
7:   For 3 <- CLR_Counter = 1
8:     Apply TS(TS_Counter) and CLR(CLR_Counter) with Image histogram to the CLAHE technique
9:     Compute DE and PSNR
10:    Compute DataSignal= DE × PSNR
11:    If DataSignal > previous DataSignal
12:      OptimumTS = TS (TS_Counter) and OptimumCLR = CLR (CLR_Counter)
13:    End If
14:   End For
15: End

```

FIGURE 4. Pseudo code to the first stage of the ACLTSHE technique.

must search for the best value (food source) of 999 suggested values (food sources). The inputs of WOA in this study were three parameters: (i) *OptimumTS*, (ii) *OptimumCLR*, and (iii) input image histogram. The fitness function of the WOA algorithm was measured as a multi-objective function to obtain non-dominant solutions of the maximum value of information richness (maxDE) and the maximum

TABLE 4. The combination of DE and PSNR of the fitness function.

Entropy (DE)	PSNR	Result
Low	Low	Fail
Low	High	Fail
High	Low	Fail
High	High	Successful

TABLE 5. Various CL, PSNR, and DE of selecting the OptimumTS.

OptimumTS	CL	PSNR	DE
8	0.0328	12.230	7.814
	0.0195	14.127	7.801
	0.0682	11.067	7.846
	0.0103	17.316	7.805

value of information signal-to-noise ratio between input and resultant images (maxPSNR). Two new variables were initialized to store the maximum value of DE (maxDE) and the maximum value of PSNR (maxPSNR) as they represent the fitness function to ensure obtaining the best local information richness without amplifying noise in the resultant image.

To avoid human dependency and intervention, ACLTSHE employs the WOA algorithm as an iterative intelligent task to adaptively and automatically obtain OptimumCL value from the selected range of OptimumCLR. The WOA algorithm spreads its agents for exploitation and exploration seeking for food source (i.e., suggested *CL*) value from input *OptimumCLR*. Next, this suggested *CL* value was applied with *OptimumTS* to the conventional CLAHE to produce an image. After that, the values of DE and PSNR factors were computed to evaluate the fitness function of this iteration. The output of the fitness function is a set of non-dominated optimum solutions in which one solution cannot improve one objective without deteriorating another. The best performance of the fitness function was attained by producing the highest DE and PSNR values.

The highest DE highlights the local details and increases information richness in the image, whereas the highest PSNR ensures the highest signal production in the resultant image by reducing or preserving the minimum error and noise due to the inverse relationship between PSNR and mean square error (MSE). Table.4 tabulates the probability of pairing both DE and PSNR to produce the fitness function of non-dominant solutions.

To explain stage two of the proposed approach, assume *OptimumTS* and *OptimumCLR* from the previous stage as (8, 0.0100). In stage two, *OptimumCL* should fall in the range of 0.0100-0.0999. Table 5 tabulates the suggested CL



(a)



(b)



(c)



(d)



(e)

FIGURE 5. Resultant image of different CL values (a) input image, (b) 0.0328, (c) 0.0195, (d) 0.0682, and (e) 0.0103.

values, along with DE and PSNR values. Figure.5 displays the visual results of the resultant images from these values, while Figure. 6 portrays the pseudo-code of the second stage.

```

1: Begin
2: Initialize WOA parameters
5: Set maxDE = 0, maxPSNR = 0, OptimumCL = 0
6: For max_iterations < iteration = 1
7:     Apply OptimumTS and CL to CLAHE
        technique
8:     Compute DE and PSNR
9:     if DE > maxDE and PSNR > max PSNR
10:        OptimumCL = CL
            maxDE = DE, maxPSNR = PSNR
11:    End if
12: End For
13: End

```

FIGURE 6. Pseudo code to the second stage of the ACLTSHE technique.

C. PRODUCING THE RESULTANT IMAGE STAGE

After obtaining *OptimumTS* and *OptimumCL* values from the previous stages, both values were applied as input variables to the standard CLAHE approach, along with the histogram of the input image to produce the output enhanced image. The applied values assure that the resultant image has highlighted local details to the maximum value with the highest information signal while preserving minimum error between the input and resultant images.

V. DATASETS AND EVALUATION METRICS

The performance of the proposed approach was assessed with 691 images of two public datasets and 8060 clinical MRI slices. These 8060 images were produced by extracting 155 slices from each 3D MRI volume data in the dataset. The first dataset called Pasadena-houses 2000 had 241 images with size 1670×1168 [60], while the second dataset is faces-1999 that contained 450 images with size 896×592 [61], and the third dataset is BraTS dataset image with each MRI 3D case image having a volume dimension of $240 \times 240 \times 155$. The 3D brain volume was used to extract 2D MRI slices with the size of 240×240 . The first and second datasets were collected from Image Processing Places, whereas the third BraTS was collected from [62]. These datasets were selected based on the wide range of information richness and the various local and hidden details found in the images. Several images of these datasets contain large uniform intensity background regions such as (sky, water, and black region of MRI) and small important ROI, while others have more detailed regions with relatively homogenous regions. This broad range of image patterns ensures that the evaluation will be performed using images of varying quality and information richness. The faces 1999, Pasadena-Houses 2000, and Brats datasets suffer from intensity inhomogeneity and over-under brightness

problems. The performance of the proposed approach was evaluated on grayscale images and compared with four state-of-the-art approaches in spatial domain derived from the CHE approach: DCLHE, IAECHE, and MVSIEHE as well as the standard CLAHE. The compared approaches were chosen due to the following reasons: (i) highlighting the local details, (ii) sub-imaging the input image, (iii) deriving from CHE, but also working in the spatial domain, and (iv) published from 2017 to 2020. The test was evaluated based on qualitative and quantitative methods to verify the superior performance of the proposed approach among the others in comparison. For the qualitative evaluation, a sample image was selected and applied to all approaches, and the result of each approach is illustrated to identify the strength and drawbacks of each approach for the human eye. Next, six quantitative performance metrics were computed to assess the statistical performance of each approach to the sample images.

Additionally, the average quantitative results were computed for all datasets individually to evaluate the average performance of the proposed approach among the compared approaches. Accordingly, the evaluation of the performance had been based on (i) contrast enhancement, (ii) information richness, (iii) signal-to-noise ratio, and (iv) distortion between input and resultant images. The seven quality parameters computed in this measurement were DE, PSNR, AMBE, SSI, CII, RMSE, and SD. The DE is used to measure the information richness of the image. The image's high entropy score indicates that it includes valuable information [27]. The AMBE stands for an approach's ability to maintain the average image brightness [9]. The PSNR factor analyses the amount of degradation based on MSE and assesses the improvement between the original and the resultant images [27]. The CII evaluates the percentage of contrast improvement in the enhanced image compared to that in the original image [63]. The SSI measures how similar the two images are. This parameter's value should lie between [0,1]. An SSI score of 1 shows that the image structure has not been distorted and that the resulting image has retained its original structure. When the SSI score is 0, a mismatch between the structures of the input and the produced images is high. A high SSI score indicates a good unaltered image structure. [9]. The RMSE represents the Root MSE between the input and the resultant images. The RMSE is inversely related to the quality of the output image. When comparing the generated image to the input image, a low RMSE value indicates that the generating image has lower distortion and higher quality in its details and information [46].

The proposed ACLTSHE approach and compared approaches were assessed on Core i7 CPU with 16 GB RAM, Windows 10, and MATLAB R2019a.

VI. RESULTS AND DISCUSSION

The proposed approach's qualitative and quantitative performances were compared with conventional CLAHE and four state-of-the-art contrast enhancement approaches; DCLHE,

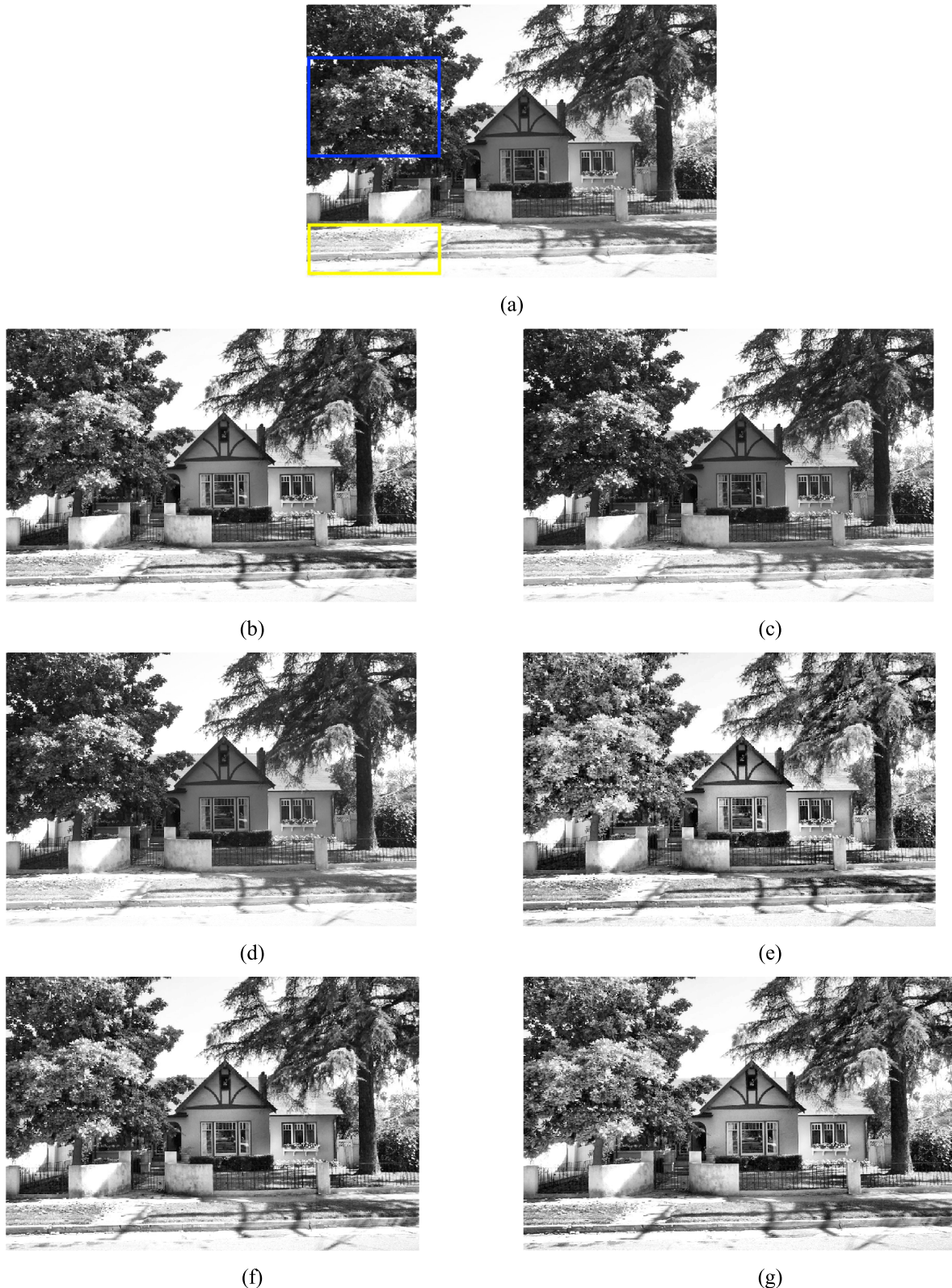


FIGURE 7. Resultant image of Pasadena-Houses 2000 sample image after applying with (a) input image, (b) DCLHE, (c) MVSIEHE, (d) IAECHE, (e) CLAHE, (f) AEIHE, and (g) ACLSTHE.

MVSIEHE, IAECHE, and AEIHE, which belong to HE, MHE, histogram-based division, and Metaheuristic categories,

respectively. The compared approaches were implemented by using their optimum input parameters as prescribed by

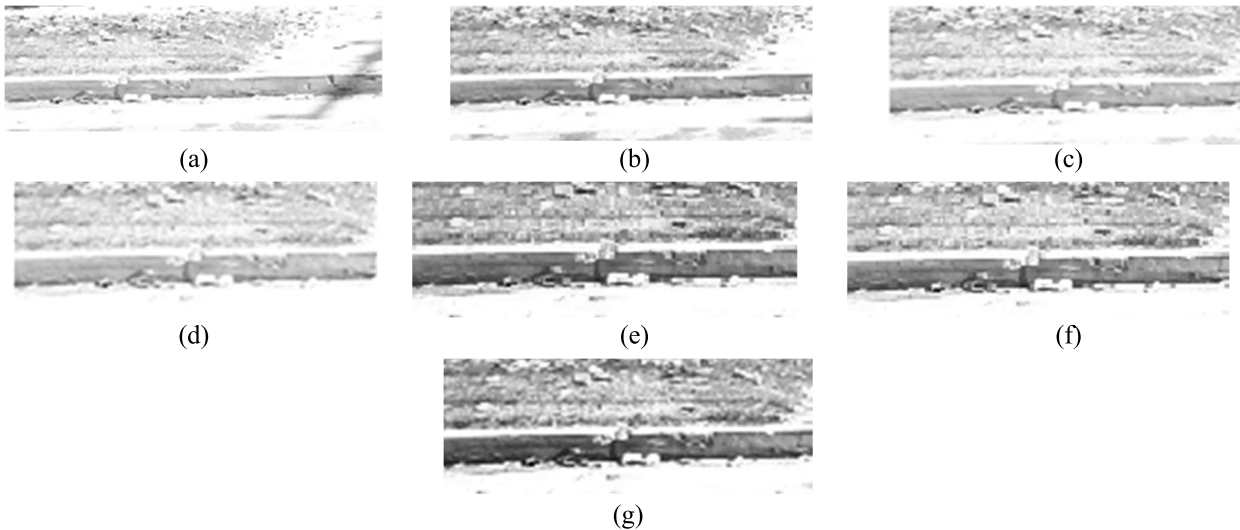


FIGURE 8. Magnified yellow area of Pasadena-Houses 2000 sample image after enhanced with (a) input image, (b) DCLHE, (c) MVIHE, (d) IAECHE, (e) CLAHE, (f) AEIHE, and (g) ACLSTHE.

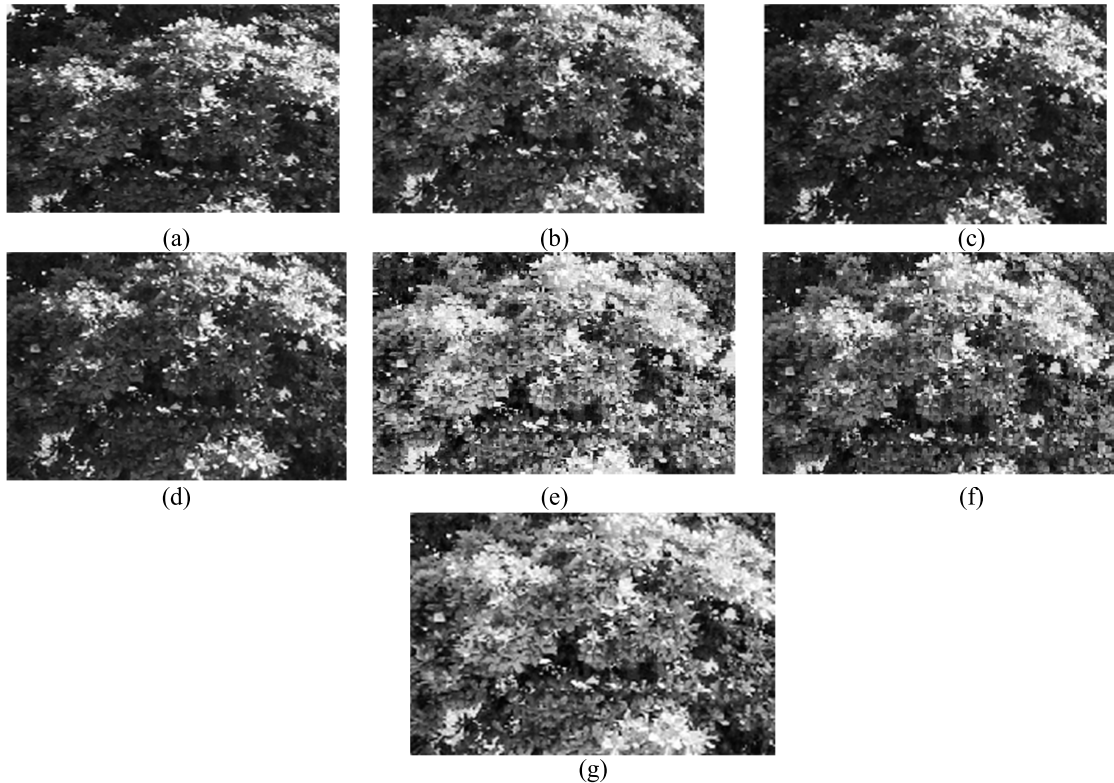


FIGURE 9. Magnified purple area of Pasadena-Houses 2000 sample image after applying with (a) input image, (b) DCLHE, (c) MVIHE, (d) IAECHE, (e) CLAHE, (f) AEIHE, and (g) ACLSTHE.

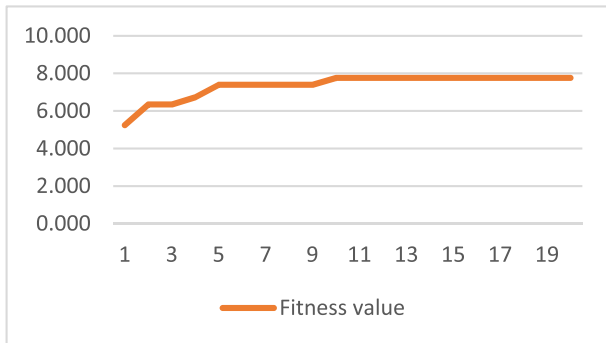
their corresponding authors. The qualitative results of the sample images from the chosen datasets are tabulated in Figures 7, 11, and 15. Figures 8 and 9 illustrate the magnified parts of the sample images derived from the Pasadena-House 2000 dataset, whereas Figures 12 and 13 display the magnified parts of the sample images retrieved from the Faces 1999 dataset. Finally, Figures 16 and 17 show

the magnified parts of the sample images extracted from the BraTS 2019 dataset. The quantitative results of all sample images are tabulated in Tables 6, 7, and 8, while the average values of all datasets are presented in Table 9.

The qualitative assessment of the sample image from Pasadena-Houses 2000 to all approaches is presented in Figure 7, while the magnified regions in yellow and blue

TABLE 6. Quantitative results of Pasadena-Houses 2000 sample image.

Approach	DE	PSNR	AMBE	SSI	CII	RMSE	SD
IAECHE	7.539	21.173	5.479	0.925	1.005	9.829	<u>77.608</u>
MVSIHE	7.290	50.559	2.049	0.995	1.006	0.756	84.900
DCLHE	7.355	<u>36.405</u>	<u>0.926</u>	0.986	1.025	<u>2.304</u>	83.668
CLAHE	<u>7.622</u>	17.619	0.877	0.777	0.989	9.588	64.946
AEIHE	7.605	21.072	6.137	0.861	0.967	9.547	81.302
ACLTSHE	7.779	20.655	7.473	<u>0.992</u>	<u>1.010</u>	7.225	80.694

**FIGURE 10.** Fitness function value iterations of Pasadena- Houses sample image.

are illustrated in Figures 8 and 9, respectively. The input image exhibited various levels of local and hidden details, such as trees leaves, fence of house garden, and street grass. Nevertheless, the image suffered from low brightness that darkened some important information. Hence, this image was selected as the sample image to evaluate the visual performance for all the approaches. The IAECHE approach failed to maintain the overall image brightness, thus did not highlight the ROI and local details of the image, such as the front area of the house, the shadow of trees on the street in front of the fence, and garden grass behind the fence (see Figure 7(d)). The magnified blue region was barely enhanced, while the details of tree leaves were barely visible, as shown in Figure 8(d). The yellow magnified region in Figure 9(d) shows that the IAECHE approach was able to highlight the borders of the street besides highlighting grass and fallen leaves. The resultant images of both MVSIHE and DCLHE approaches were barely enhanced, and the image low brightness issue was left unresolved, such as that noted at the house main entrance, tree details, and garden details in front of the house (see Figures 7(b) & (c)). Moreover, the resultant image of the CLAHE technique is not pleasant to the human eyes due to the over contract drawback, as illustrated in Figure 7(e). The magnified regions of the CLAHE technique in Figures 8(e) and 9(e) also suffer from various artifacts and noise amplification, which leads to a corrupted ROI in the resultant images. While the resultant image of the AEIHE technique could not prove its capability

to highlight the local details of the image, such as the main door of the house fence, as illustrated in Figure 7(f). The yellow and blue magnified regions in Figures 8(f) and 9(f) show that the AEIHE approach highlighted tree leaves' details and the street's borders besides highlighting grass and fallen leaves.

Clearly, the resultant image of the proposed ACLTSHE approach displayed superiority to the other compared approaches, which not only solved the issue of low brightness and highlighted the local details, but also the resultant image was pleasant and clear to the human eye. Accordingly, the front side of the house and the garden details are well presented in Figure 7(g). The high improvement performance of the approach appeared clear on the magnified blue and yellow regions as they were enhanced in an optimum manner. For instance, the details of the leaves were present and highlighted, while the street border was improved, and both the grass and leaves were clearer than the other compared approaches (see Figure 8(g) & Figure 9(g)).

To support the qualitative assessment, the seven quantitative factors were computed for all approaches and tabulated in Table 6. The quantitative data clearly justify that the proposed ACLTSHE approach could produce the best information richness and second-best similarity structure and contrast improvement of the resultant image. Thus, highlighting the local details as the DE value was the best among the other approaches. Despite the CLAHE approach generated the second-best DE value but suffered from over-contrast issues, as illustrated in Figure 7(e). The consequences of these two numbers proved the drawbacks of DCLHE and MVSIHE approaches in highlighting or even preserving the image details. The low performance of DCLHE and MVSIHE in highlighting the local details is reflected on RMSE. The low values of RMSE of these approaches refer to the small variance between input and resultant images due to the slight modification and manipulation made to the intensity of the image details. These small values impacted the PSNR value as the PSNR was directly related to the MSE (small MSE value generated high PSNR value). The small enhancement on the image negatively impacted the brightness aspect, which led to less brightness enhancement (see Table.5). Notably, DCLHE produced the best AMBE value, while the MVSIHE generated the second-best value. Meanwhile,



FIGURE 11. Resultant image of faces 1999 sample image after enhanced with (a) input image, (b) DCLHE, (c) MVIHE, (d) IAECHE, (e) CLAHE, (f) AEIHE, and (g) ACLTSHE.

the proposed ACLTSHE approach proved its capability to preserve the image's structure by producing the best SSI value compared to the rest. The DCLHE approach produced the second-best value of the SSI parameter. For CII, the values of

all approaches were close, yet the proposed ACLTSHE and the DCLHE approaches yielded the best and the second-best results, respectively. Additionally, the ACLTSHE approach could produce the second-best CII, which displayed the

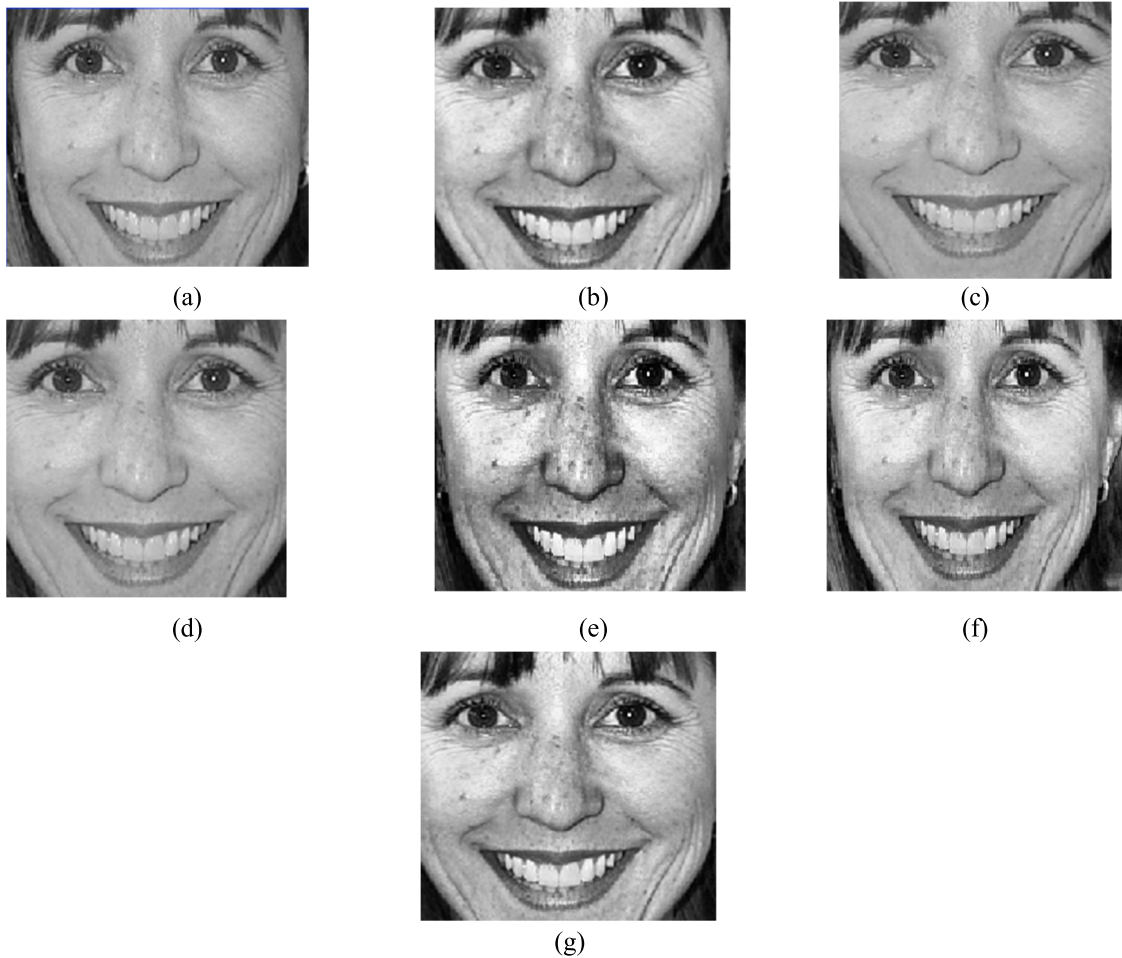


FIGURE 12. Magnified yellow area of faces 1999 sample image after enhanced with (a) input image, (b) DCLHE, (c) MVSIE, (d) IAECHE, (e) CLAHE, (f) AEIHE, and (g) ACLSTHE.

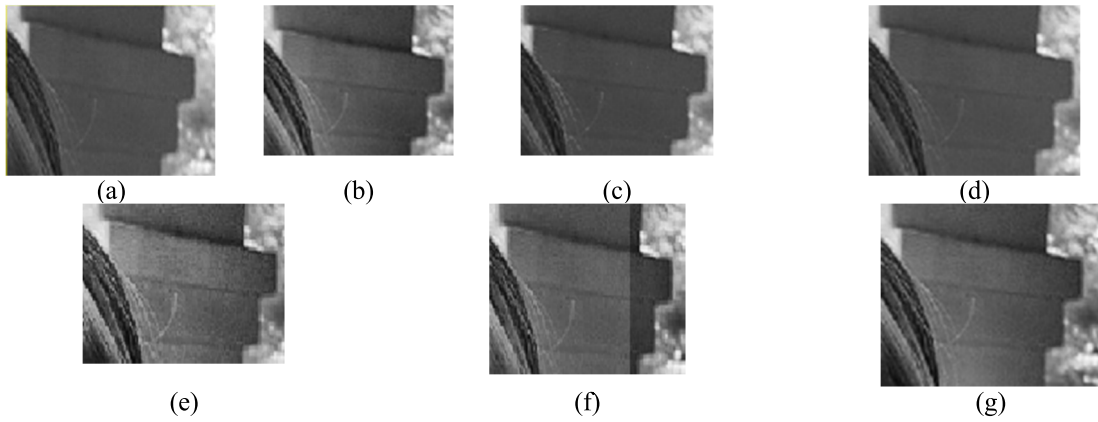


FIGURE 13. Magnified purple area of faces 1999 sample image after applying with (a) input image, (b) DCLHE, (c) MVSIE, (d) IAECHE, (e) CLAHE, (f) AEIHE, and (g) ACLSTHE.

superior capability of the proposed ACLTSHE approach to control the contrast improvement of the image without distortion and noise amplification.

Additionally, Figure 10 illustrates the fitness function value of each iteration of the proposed technique. In this Figure, the number of iterations is limited to 20. The fitness

value of the proposed technique changed its value a few times until it stacked with the best value according to the best value that matches equation (1).

The sample images of the faces dataset are displayed in Figure 11(a). This image suffers from multiple drawbacks, such as blurry background, vanished face aging details,

TABLE 7. Quantitative results of Faces 1999 sample image.

Approaches	DE	PSNR	AMBE	SSI	CII	RMSE	SD
IAECHE	7.756	22.191	1.772	0.928	1.007	9.173	<u>60.348</u>
MVSIHE	7.481	<u>36.405</u>	0.134	0.986	1.025	<u>2.304</u>	62.168
DCLHE	7.593	50.559	<u>0.571</u>	0.999	1.000	0.756	60.064
CLAHE	<u>7.822</u>	17.619	0.877	0.777	0.989	9.588	64.946
AEIHE	7.749	21.707	2.880	0.826	0.996	9.406	61.633
Proposed ACLTSHE	7.924	28.368	2.002	<u>0.983</u>	<u>1.023</u>	4.973	66.502

**FIGURE 14.** Fitness function value iterations of Faces 1999 sample image.

and the degree of hair color of the woman. Therefore, the proposed ACLSTHE approach and the other compared approaches were applied to enhance this image to test their capability to improve the visual image representation. The resultant images of the IAECHE, AEIHE, and ACLSTHE approaches were obviously enhanced, and the details of the images were highlighted very well. The grass behind the woman was highlighted, and the leaves details were well presented, as shown in Figures 11(d), (f), and (g). The approaches proved their capability to demonstrate the degrees of the hair color. However, the superiority of the proposed ACLSTHE approach was presented in the magnified regions (yellow & blue regions). The ACLTSHE approach brightened the image more than the IAECHE and AEIHE approaches especially the woman's face. Although the wall bricks behind the woman suffered from dimming issue, the ACLTSHE approach was able to brighten this region better than the IAECHE and AEIHE approaches and without distorting the other regions (see Figure 12(g)). The three approaches were able to highlight the face details, such as the aging lines around the woman's eyes, the spots on her nose, and the mouth details of the woman (see Figures 13 (d) (f) & (g)).

Meanwhile, both DCLHE and MVSIHE approaches failed to highlight the local details or reduce the blur impact of the image, whereby the resultant images were unpleasant to the human eye. The woman's hair color had barely improved, and the grass in the background had vanished. Both the approaches kept the darkening effect and failed to brighten the image, as shown in Figures 11 (b) and (c), respectively.

The magnified regions of the input image were not improved or even preserved, such as the wall bricks behind the woman in the yellow magnified region. The aging details around the eyes and mouth or the spots on the nose have also reflected the drawbacks of these approaches in maintaining the hidden details, as presented in Figures 12 (b) & (c) and Figures 13 (b) & (c). The quantitative results of the faces 1999 sample image are tabulated in Table 7. The information richness value (DE parameter) of the proposed ACLSTHE approach displayed its superior capability to enhance the details of the input image, thus generating a resultant image with the local details highlighted due to the best DE value retrieved. The CLAHE and IAECHE approaches also enhanced the local details by producing the second and third-best DE values. Although the proposed approach did not yield the highest PSNR value, it was capable of maintaining the structural similarity between input and resultant images due to the close values of the SSI parameter of all approaches in reaching perfection (value 1). The contrast improvement was remarkable when compared with the other approaches. This proved that the approach could highlight local and hidden details despite failing to score the best RMSE and PSNR values. Both MVSIHE and DCLHE approaches yielded the best and the second-best values of AMBE, respectively, but failed to solve the darkening issue or distinguish the ROI between foreground and background regions. Despite AEIHE could enhance the sample image qualitatively but failed to compete with other quantitative approaches.

Additionally, Figure 14 illustrates the fitness function value of each iteration of the proposed technique. In this Figure, the number of iterations is limited to 20. The fitness value of the proposed technique changed its value a few times until it stacked with the best value according to the best value that matches equation (1).

Sample Image 3 was selected from the BraTS 2019 dataset. This sample image suffered from intensity inhomogeneity that led to over brightness and poor local details. Thus, the sample image was enhanced by applying the proposed approach and the three compared approaches. Referring to Figure 15, The resultant images of the CLAHE, AEIHE, and ACLSTHE approaches were enhanced qualitatively, and the details of the images were highlighted very well. However, the resultant images of the CLAHE suffer from

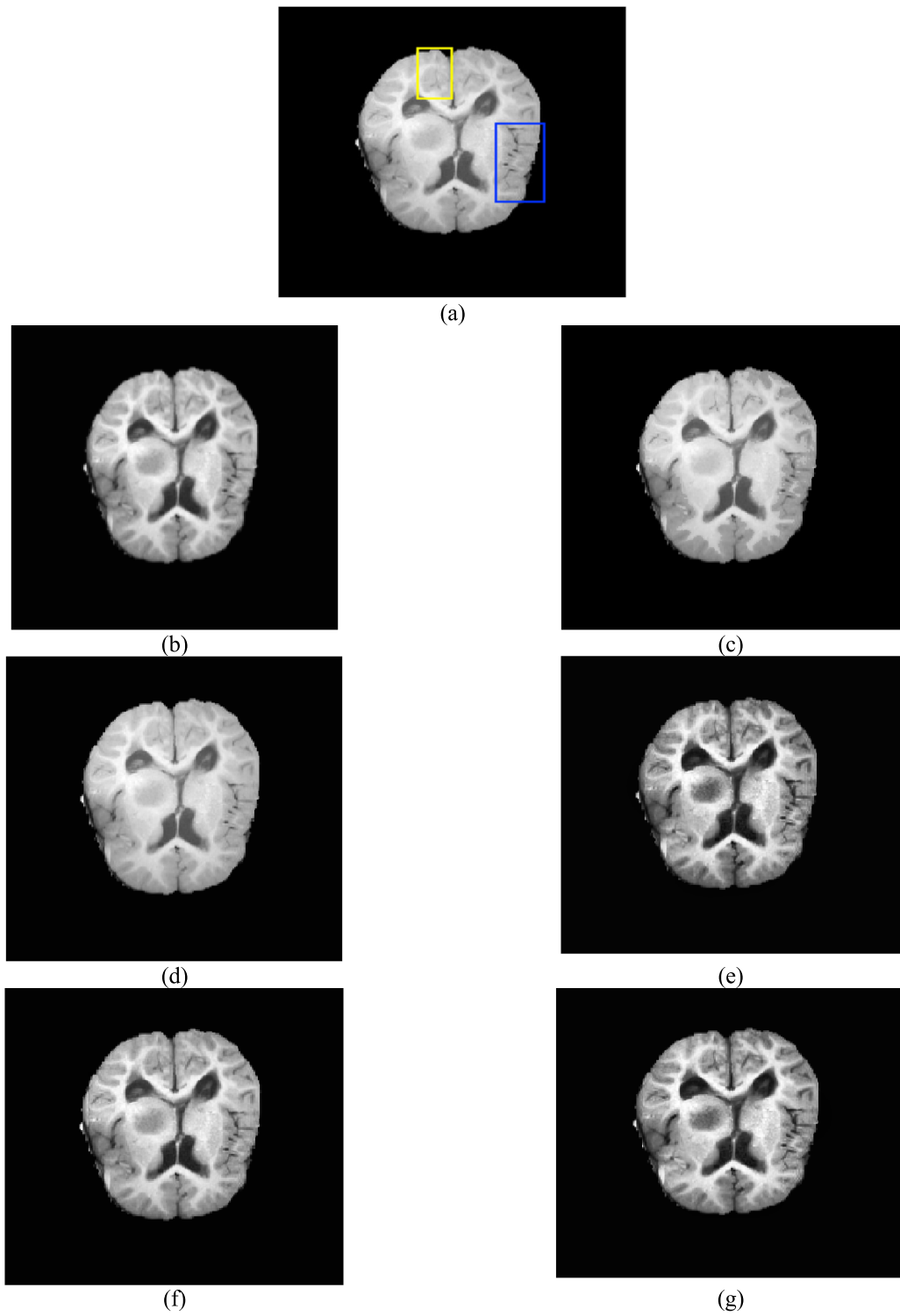


FIGURE 15. Resultant image of BraTS 2019 sample image after applying with (a) input image, (b) DCLHE, (c) MVSIEHE, (d) IAECHE, (e) CLAHE, (f) AEIHE, and (g) ACLSTHE.

over enhancement issues, leading to omitting the small important details. The resultant image of the proposed approach displayed its superior capability among the other approaches to enhance and highlight the image's details,

as shown in Figure 15(g). This approach had isolated the regions in the brain based on the diversity of the gray levels, thus producing a pleasant and natural resultant image. The yellow and blue magnified regions in the input image suffered

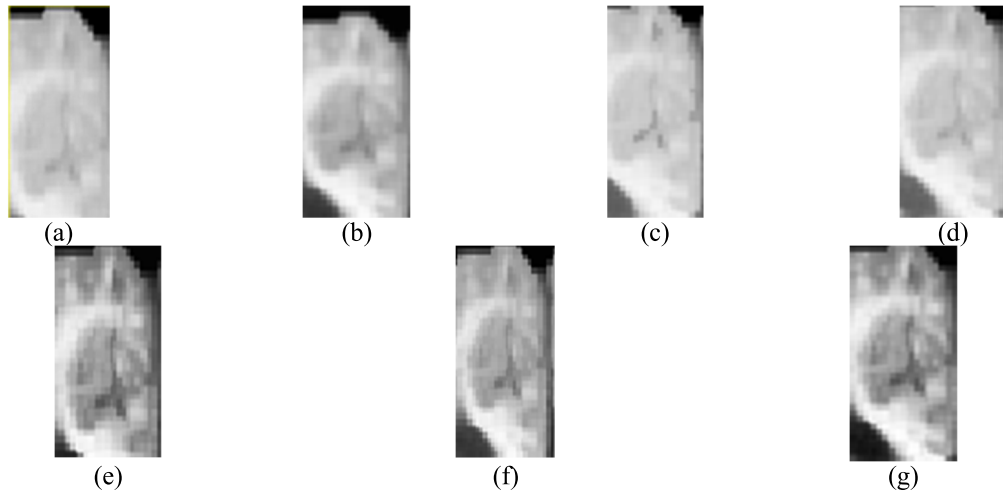


FIGURE 16. Magnified yellow area of BraTS 2019 sample image after enhanced with (a) input image, (b) DCLHE, (c) MVSIE, (d) IAECHE, (e) CLAHE, (f) AEIHE, and (g) ACLSTHE.

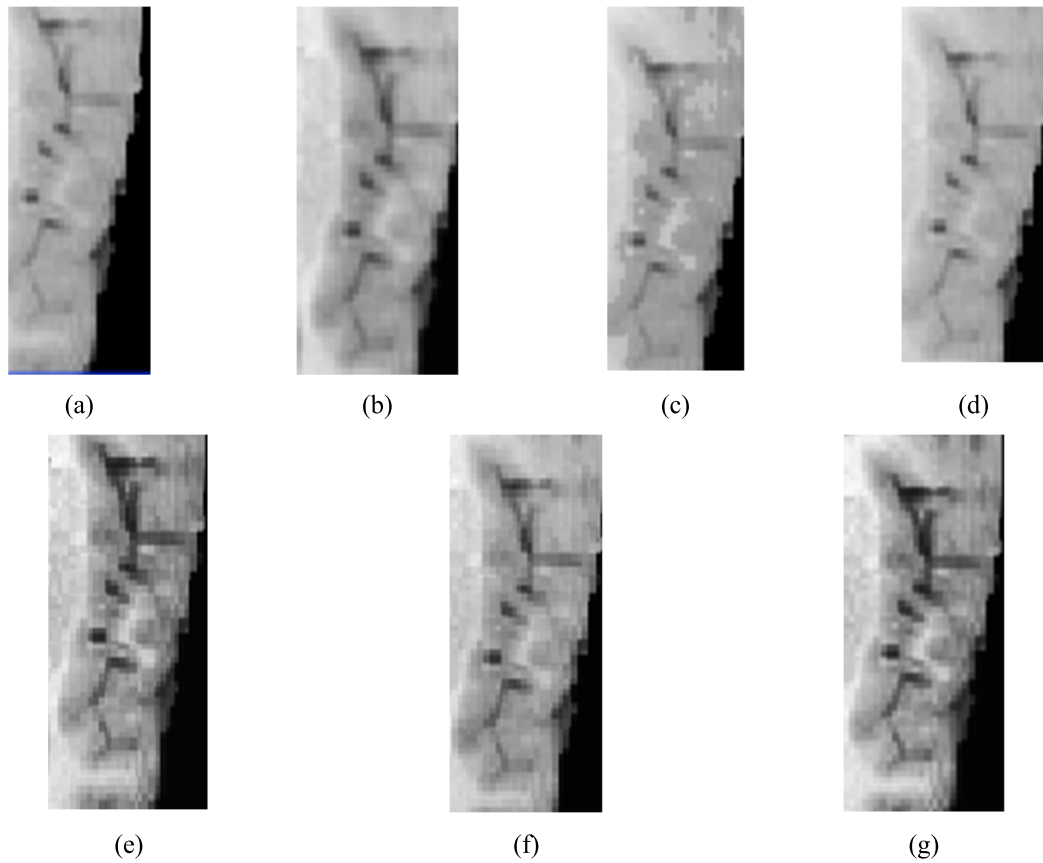


FIGURE 17. Magnified purple area of BraTS 2019 sample image after enhanced with (a) input image, (b) DCLHE, (c) MVSIE, (d) IAECHE, (e) CLAHE, (f) AEIHE, and (g) ACLSTHE.

from hidden details issue, while the ACLTSHE approach had successfully highlighted the local details and widened the difference between the brain tissues (i.e., white matter, grey matter, and cerebrospinal fluid) in these two regions, as shown in Figure 16(g) and Figure 17(g). The IAECHE approach enhanced the brain sample image and highlighted the local details, but the quality and the naturalness of the

resultant image were poorer than those of the proposed ACLTSHE approach (see Figure 15(d)). The magnified regions (yellow & blue) presented in Figure 16(d) and Figure 17(d) illustrate a difference and improvement in these two regions. The resultant images of DCLHE and MVSIE approaches displayed in Figures 15 (b) and (c), respectively, were barely enhanced from the input images.

TABLE 8. Quantitative results of BraTS 2019 sample image.

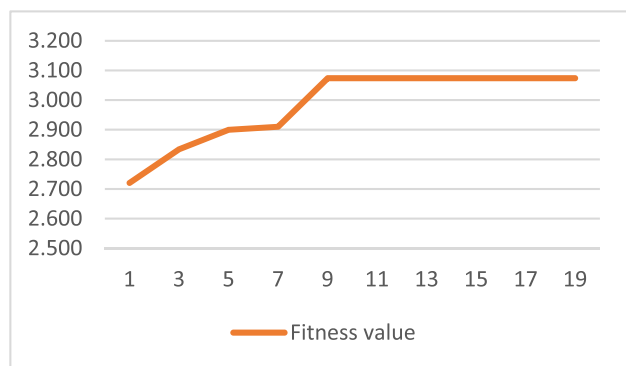
Technique	DE	PSNR	AMBE	SSI	CII	RMSE	SD
IAECHE	3.016	29.564	<u>1.028</u>	0.716	0.985	2.804	79.151
MVSIHE	2.811	<u>37.854</u>	1.109	0.992	0.893	1.979	85.210
DCLHE	2.855	41.956	2.013	<u>0.733</u>	0.976	<u>2.035</u>	85.206
CLAHE	<u>3.043</u>	21.711	4.109	0.467	0.955	3.915	<u>75.334</u>
AEIHE	3.000	26.539	2.594	0.717	1.022	2.837	80.046
Proposed ACLTSHE	3.085	22.294	4.971	0.704	<u>0.998</u>	3.461	75.298

This proved the limitation of these approaches to highlight the local details and to optimize the appearance of brain tissue, thus cannot easily distinguish the tumor regions in the brain tissue. The magnified regions could be hardly noted for these approaches, as shown in Figures 16(b) & (c) and Figures 17(b) & (c). Table.8 tabulates the quantitative results of the sample image. The proposed ACLTSHE approach produced the best DE value, which indicated its capability to allocate the local detail regions in the image and enhance them. Besides, the approach had successfully improved image contrast and controlled the over contrast issue by producing the best CII value.

Furthermore, the image's background (i.e., the black color) did not affect the foreground region (brain tissue) during the enhancement process and did not raise the image's darkness. Although the second-best value of DE reported by the CLAHE approach showed its capability to highlight and enhance the local details, it failed to preserve the image structure as the produced low value of the SSI parameter denotes high distortion in the resultant image when compared with the input image. Next, the IAECHE approach generated the second and third-best AMBE and DE values, respectively, showing its ability to enhance local details and maintain the average image brightness. Due to the enhancement drawback of the MVSIHE approach, it produced the best RMSE value that led to a small error value between input and resultant images. The RMSE value influenced the PSNR to attain the second-best value. This approach maintained the image's brightness and structure by producing the best AMBE and SSI values.

The DCLHE approach preserved the second-best RMSE value, scoring the best PSNR value to enlarge the signal information without amplifying noise. Finally, the AEIHE approach produced the best CII value, showed its capability to improve image contrast, and controlled the over-contrast issue.

Additionally, Figure 18 illustrates the fitness function value of each iteration of the proposed technique. In this Figure, the number of iterations is limited to 20. The fitness value of the proposed technique changed its value a few times until it stacked with the best value according to the best value that matches equation (1).

**FIGURE 18.** Fitness function value iterations of BraTS 2019 sample image.

The performance of the proposed approach and the compared approaches were also evaluated by computing the average value of all the quantitative parameters for all the datasets images. The average values of DE, PSNR, AMBE, SSI, CII, and RMSE were computed for 241, 450, and 8060 images derived from Pasadena-houses 2000, faces 1999, and BraTS 2019 datasets, respectively, (see Table 9).

The proposed approach proved its superior capability to improve information richness and contrast improvement for the Pasadena-Houses 2000 dataset, mainly due to its best DE and CII values of 7.658 and 1.021, respectively. The two values proved the capability of the proposed approach to highlight local details and control the over-contrast of the input image. Meanwhile, the CLAHE approach yielded 7.752 and 1.015 as the second-best values for DE and CII, respectively. Next, the MVSIHE approach generated the best AMBE value and the second-best values of PSNR, SSI, and RMSE, respectively, whereas the DCLHE approach produced the best PSNR, SSI, and RMSE values, as well as the second-best AMBE value. Although the CLAHE technique produced the second-best average DE and the best average SD values of the datasets, it could not produce natural and pleasant enhanced images. The IAECHE approach produced the second-best average SD values of the datasets. The AEIHE failed to compete with the other approaches for all quantitative parameters of the enhancement process of the datasets.

TABLE 9. The average quantitative results for Pasadena-Houses 2000, Faces 1999, and BraTS 2019 datasets.

Dataset	Technique	DE	PSNR	AMBE	SSI	CII	RMSE	SD
Pasadena-Houses 2000	IAECHE	7.623	22.770	6.706	0.936	1.013	9.198	<u>72.879</u>
	MVSIHE	7.330	<u>38.259</u>	1.259	<u>0.991</u>	1.010	<u>1.705</u>	76.320
	DCLHE	7.465	44.331	<u>1.468</u>	0.998	0.999	1.557	74.302
	AEIHE	7.639	21.627	7.265	0.892	0.984	9.574	73.887
	CLAHE	<u>7.752</u>	17.706	12.055	0.764	<u>1.015</u>	10.587	60.296
	Proposed ACLTSHE	7.658	20.750	9.078	0.882	1.021	9.750	74.836
Faces 1999	IAECHE	7.609	23.386	7.269	<u>0.939</u>	1.020	9.364	58.018
	MVSIHE	7.297	21.424	1.609	0.984	<u>1.021</u>	9.741	60.712
	DCLHE	7.482	42.853	<u>2.106</u>	0.997	1.000	2.075	<u>58.347</u>
	AEIHE	<u>7.636</u>	22.337	7.299	0.873	0.980	9.554	58.837
	CLAHE	7.306	17.071	12.638	0.797	1.012	10.646	71.814
	Proposed ACLTSHE	7.686	<u>35.871</u>	9.025	0.900	1.026	<u>3.363</u>	61.207
BraTS 2019	IAECHE	2.710	27.317	4.866	0.799	0.994	6.126	56.034
	MVSIHE	2.760	36.195	1.043	<u>0.818</u>	1.000	3.582	59.881
	DCLHE	2.663	<u>34.309</u>	<u>3.953</u>	0.714	<u>0.997</u>	<u>4.412</u>	<u>58.414</u>
	AEIHE	<u>2.903</u>	27.339	4.202	0.695	1.000	5.849	61.265
	CLAHE	2.656	23.065	7.618	0.423	0.963	6.836	58.600
	Proposed ACLTSHE	2.915	26.663	4.179	0.986	0.984	4.959	59.998

TABLE 10. Average processing time in seconds of the compared techniques.

Technique	Pasadena-Houses 2000	Faces 1999	BraTS 2019
IAECHE	30.0	23.4	12.0
MVSIHE	3.0	3.4	10.3
DCLHE	4.3	3.0	13.3
AEIHE	103.0	87.5	69.3
CLAHE	6.0	7.0	3.0
Proposed ACLTSHE	79.0	66.3	65.3

The proposed ACLTSHE approach was the best approach that enhanced information richness and contrast with DE and CII values of 7.686 and 1026, respectively, for the faces 1999 dataset. The proposed approach yielded the second-best PSNR and RMSE values of 35.871 and 3.363, respectively. These values proved the superior performance of the proposed ACLTSHE approach over the rest in highlighting the local details and improving the image

signals without amplifying the noise or generating undesired artifacts. The proposed approach reduces the additive high-frequency noise in the resultant images by adaptively and automatically clipping the input image's histogram at a predefined value extracted locally before computing the cumulative distribution function. The IAECHE approach produced the best SD, second-best DE, and CII average values. The MVSIHE approach preserved the average brightness of the dataset as it attained the best AMBE value. This approach had successfully preserved the structure of the image by producing the second-best SSI value.

Meanwhile, the DCLHE approach yielded the best PSNR, RMSE, SSI, and the second-best AMBE value compared to the other approaches. The AEIHE approach produced the second-best average DE value. Meanwhile, the AEIHE approach could not compete with other techniques for all quantitative metrics of the enhancement process.

As for the BraTS 2019 dataset, the best DE and SSI values were generated by the proposed ACLTSHE approach (2.915 and 0.986, respectively), while the AEIHE approach produced the second-best DE value. The MVSIHE approach yielded the best PSNR, AMBE, CII, and RMSE values, whereas the DCLHE approach produced the second-best values of these parameters. The IAECHE failed

to compete with the other approaches for the enhancement process for all parameters except the SD as it was able to produce the best value among the other techniques, thus displaying its shortcoming related to the limited range of grayscale. The average values tabulated in Table 9 validate the analysis and assume that the proposed ACLTSHE approach displayed the superior capability to highlight local and hidden details in the image. The average processing time to enhance the images of the datasets of the proposed ACLTSHE technique and all other compared is tabulated in Table 10. As shown in this Table, the AEIHE approach reports the longest average running time among all the compared approaches, which took 103.0, 87.5, 69.3 seconds for enhancing the images of three datasets: Pasadena-houses 2000, faces 1999, and BraTS 2019, respectively. The proposed approach was the second longest-average running time among compared approaches, which took 79.0, 66.3, 65.3 for enhancing the images of the three datasets. On the other hand, the shortest-average running time was reported by the MVIHE approach, which took 3.0 seconds for enhancing the images of Pasadena-houses 2000, while the DCLHE and CLAHE approaches report the best running time for enhancing the samples images of two datasets: faces 1999 and BraTS 2019, which took 3.0 seconds.

VII. CONCLUSION

This paper proposes a new adaptive and automatic version of the CLAHE-based contrast enhancement approach called ACLTSHE to tackle the subjective effects of manual parameter setting values by computing the optimum CL range and tile size automatically and adaptively.

A new fitness function termed DataSignal is proposed to attain optimum entropy and to preserve optimum information signal value. The proposed approach was evaluated using the Pasadena-houses 2000 dataset, faces 1999, and BraTS 2019 datasets. Qualitative and quantitative results have shown that the ACLTSHE approach yields competitive performance in three different datasets. Especially in BraTS 2019, the contrast enhancement performances are outperformed comparison approaches based on average DE and SSI. The achieved high DE value by the ACLTSHE approach demonstrated its capability to enhance images and produce a high-quality resultant image.

The ACLTSHE approach had successfully maintained the image's original structure and increased information signal without undesired distortion and noise amplification of resultant images. Overall, the ACLTSHE approach has displayed its ability to enhance the contrast, highlight details, and preserve the structure similarity of input and resultant images, thus highlighting its potential for applications in medical imaging and industrial fields.

As the ACLTSHE model reported the second-longest-running time among the compared approaches, the ACLTSHE is inappropriate for real-time image enhancement applications. In the future, we will explore an improvement to the ACLTSHE to be used for timely image enhancement

applications. Two possible solutions can be performed to overcome or reduce the time complexity. First, the searchability of the WOA can be improved by attaching adaptive nonlinear convergence parameters to the original algorithm. Second, the ACLTSHE approach can be adaptively improved to determine the optimal number of enhancement iterations for each tile size to obtain the best fitness values by fully utilizing every iteration. Besides, the proposed technique is limited to being applied to gray-level images in its current form. Therefore, improving the ACLTSHE to be used for enhancing colored images is also our future work.

REFERENCES

- [1] P. Suganya, S. Gayathri, and N. Mohanapriya, "Survey on image enhancement techniques," *Int. J. Comput. Appl. Technol. Res.*, vol. 2, no. 5, pp. 623–627, Sep. 2013, doi: [10.7753/ijcatr0205.1019](https://doi.org/10.7753/ijcatr0205.1019).
- [2] A. Fawzi, A. Achuthan, and B. Belaton, "Brain image segmentation in recent years: A narrative review," *Brain Sci.*, vol. 11, no. 8, p. 1055, Aug. 2021, doi: [10.3390/brainsci11081055](https://doi.org/10.3390/brainsci11081055).
- [3] H. Lidong, Z. Wei, W. Jun, and S. Zebin, "Combination of contrast limited adaptive histogram equalisation and discrete wavelet transform for image enhancement," *IET Image Process.*, vol. 9, no. 10, pp. 908–915, Oct. 2015, doi: [10.1049/iet-ipr.2015.0150](https://doi.org/10.1049/iet-ipr.2015.0150).
- [4] R. C. Gonzalez, R. E. Woods, and S. L. Eddins, *Digital Image Processing*, vol. 2, 2nd ed. Upper Saddle River, NJ, USA: Prentice-Hall, 2002.
- [5] S. Dipppel, M. Stahl, R. Wiemker, and T. Blaffert, "Multiscale contrast enhancement for radiographies: Laplacian pyramid versus fast wavelet transform," *IEEE Trans. Med. Imag.*, vol. 21, no. 4, pp. 343–353, Apr. 2002, doi: [10.1109/TMI.2002.1000258](https://doi.org/10.1109/TMI.2002.1000258).
- [6] M. Agarwal and R. Mahajan, "Medical image contrast enhancement using range limited weighted histogram equalization," *Proc. Comput. Sci.*, vol. 125, pp. 149–156, Jan. 2018, doi: [10.1016/j.procs.2017.12.021](https://doi.org/10.1016/j.procs.2017.12.021).
- [7] K. Singh and R. Kapoor, "Image enhancement using exposure based sub image histogram equalization," *Pattern Recognit. Lett.*, vol. 36, pp. 10–14, Jan. 2014, doi: [10.1016/j.patrec.2013.08.024](https://doi.org/10.1016/j.patrec.2013.08.024).
- [8] W. Z. W. Ismail and K. S. Sim, "Contrast enhancement dynamic histogram equalization for medical image processing application," *Int. J. Imag. Syst. Technol.*, vol. 21, no. 3, pp. 280–289, 2011, doi: [10.1002/ima.20295](https://doi.org/10.1002/ima.20295).
- [9] H. Ibrahim and N. S. P. Kong, "Brightness preserving dynamic histogram equalization for image contrast enhancement," *IEEE Trans. Consum. Electron.*, vol. 53, no. 4, pp. 1752–1758, Nov. 2007, doi: [10.1109/TCE.2007.4429280](https://doi.org/10.1109/TCE.2007.4429280).
- [10] R. C. Gonzalez and R. E. Woods, *Digital Image Processing Using MATLAB*, 2nd ed. London, U.K.: Pearson Education, 2004.
- [11] Y.-T. Kim, "Contrast enhancement using brightness preserving bi-histogram equalization," *IEEE Trans. Consum. Electron.*, vol. 43, no. 1, pp. 1–8, Feb. 1997, doi: [10.1109/30.580378](https://doi.org/10.1109/30.580378).
- [12] M. Abdullah-Al-Wadud, "A modified histogram equalization for contrast enhancement preserving the small parts in images," *Int. J. Comput. Sci. Netw. Secur.*, vol. 12, no. 2, pp. 1–4, 2012.
- [13] S. F. Tan and N. A. M. Isa, "Exposure based multi-histogram equalization contrast enhancement for non-uniform illumination images," *IEEE Access*, vol. 7, pp. 70842–70861, 2019, doi: [10.1109/ACCESS.2019.2918557](https://doi.org/10.1109/ACCESS.2019.2918557).
- [14] J. R. Tang and N. A. M. Isa, "Intensity exposure-based bi-histogram equalization for image enhancement," *TURKISH J. Electr. Eng. Comput. Sci.*, vol. 24, no. 5, pp. 3564–3585, 2016.
- [15] N. H. Saad, N. A. M. Isa, and H. M. Saleh, "Nonlinear exposure intensity based modification histogram equalization for non-uniform illumination image enhancement," *IEEE Access*, vol. 9, pp. 93033–93061, 2021, doi: [10.1109/ACCESS.2021.3092643](https://doi.org/10.1109/ACCESS.2021.3092643).
- [16] J. B. Zimmerman, S. M. Pizer, E. V. Staab, J. R. Perry, W. McCartney, and B. C. Brenton, "An evaluation of the effectiveness of adaptive histogram equalization for contrast enhancement," *IEEE Trans. Med. Imag.*, vol. 7, no. 4, pp. 304–312, Dec. 1988, doi: [10.1109/42.14513](https://doi.org/10.1109/42.14513).
- [17] J.-Y. Kim, L.-S. Kim, and S.-H. Hwang, "An advanced contrast enhancement using partially overlapped sub-block histogram equalization," *IEEE Trans. Circuits Syst. Video Technol.*, vol. 11, no. 4, pp. 475–484, Apr. 2001, doi: [10.1109/76.915354](https://doi.org/10.1109/76.915354).
- [18] K. Zuiderveld, *Contrast Limited Adaptive Histogram Equalization*. San Diego, CA, USA: Academic, 1994.

- [19] P. Tao, Y. Pei, M. Celenk, Q. Fu, and A. Wu, "Adaptive image enhancement method using contrast limitation based on multiple layers BOHE," *J. Ambient. Intell. Humanized Comput.*, vol. 11, no. 11, pp. 5031–5043, Nov. 2020, doi: [10.1007/s12652-020-01810-9](https://doi.org/10.1007/s12652-020-01810-9).
- [20] V. Stumper, S. Bauer, R. Ernstorfer, B. Schölkopf, and R. P. Xian, "Multidimensional contrast limited adaptive histogram equalization," *IEEE Access*, vol. 7, pp. 165437–165447, 2019, doi: [10.1109/ACCESS.2019.2952899](https://doi.org/10.1109/ACCESS.2019.2952899).
- [21] R. Gonzalez, R. C. Gonzalez, and R. E. Woods, *Digital Image Processing*. New York, NY, USA: Pearson, 2018.
- [22] Z. Xu, X. Liu, and X. Chen, "Fog removal from video sequences using contrast limited adaptive histogram equalization," in *Proc. Int. Conf. Comput. Intell. Softw. Eng.*, Dec. 2009, pp. 3–6, doi: [10.1109/CISE.2009.5366207](https://doi.org/10.1109/CISE.2009.5366207).
- [23] Y. Wang, Q. Chen, and B. Zhang, "Image enhancement based on equal area dualistic sub-image histogram equalization method," *IEEE Trans. Consum. Electron.*, vol. 45, no. 1, pp. 68–75, Feb. 1999, doi: [10.1109/30.754419](https://doi.org/10.1109/30.754419).
- [24] S.-D. Chen and A. R. Ramli, "Minimum mean brightness error bi-histogram equalization in contrast enhancement," *IEEE Trans. Consum. Electron.*, vol. 49, no. 4, pp. 1310–1319, Nov. 2003, doi: [10.1109/TCE.2003.1261234](https://doi.org/10.1109/TCE.2003.1261234).
- [25] K. G. Dhal and S. Das, "Combination of histogram segmentation and modification to preserve the original brightness of the images," *Pattern Recognit. Image Anal.*, vol. 27, no. 2, pp. 200–212, Apr. 2017, doi: [10.1134/S1054661817020031](https://doi.org/10.1134/S1054661817020031).
- [26] C. Zuo, Q. Chen, and X. Sui, "Range limited bi-histogram equalization for image contrast enhancement," *Optik*, vol. 124, no. 5, pp. 425–431, Mar. 2013, doi: [10.1016/j.ijleo.2011.12.057](https://doi.org/10.1016/j.ijleo.2011.12.057).
- [27] L. Zhuang and Y. Guan, "Image enhancement via subimage histogram equalization based on mean and variance," *Comput. Intell. Neurosci.*, vol. 2017, pp. 1–12, Dec. 2017, doi: [10.1155/2017/6029892](https://doi.org/10.1155/2017/6029892).
- [28] K. G. Dhal, A. Das, S. Ray, J. Gálvez, and S. Das, "Histogram equalization variants as optimization problems: A review," *Arch. Comput. Methods Eng.*, vol. 28, no. 3, pp. 1471–1496, May 2021, doi: [10.1007/s11831-020-09425-1](https://doi.org/10.1007/s11831-020-09425-1).
- [29] E. Reddy and R. Reddy, "Dynamic clipped histogram equalization technique for enhancing low contrast images," *Proc. Nat. Acad. Sci., India A, Phys. Sci.*, vol. 89, no. 4, pp. 673–698, Dec. 2019, doi: [10.1007/s40010-018-0530-6](https://doi.org/10.1007/s40010-018-0530-6).
- [30] M. F. Khan, D. Goyal, M. M. Nofal, E. Khan, R. Al-Hmouz, and E. Herrera-Viedma, "Fuzzy-based histogram partitioning for bi-histogram equalisation of low contrast images," *IEEE Access*, vol. 8, pp. 11595–11614, 2020, doi: [10.1109/ACCESS.2020.2965174](https://doi.org/10.1109/ACCESS.2020.2965174).
- [31] L. Bai, W. Zhang, X. Pan, and C. Zhao, "Underwater image enhancement based on global and local equalization of histogram and dual-image multi-scale fusion," *IEEE Access*, vol. 8, pp. 128973–128990, 2020, doi: [10.1109/ACCESS.2020.3009161](https://doi.org/10.1109/ACCESS.2020.3009161).
- [32] K. S. Sim, C. P. Tso, and Y. Y. Tan, "Recursive sub-image histogram equalization applied to gray scale images," *Pattern Recognit. Lett.*, vol. 28, no. 10, pp. 1209–1221, Jul. 2007, doi: [10.1016/j.patrec.2007.02.003](https://doi.org/10.1016/j.patrec.2007.02.003).
- [33] S.-D. Chen and A. R. Ramli, "Contrast enhancement using recursive mean-separate histogram equalization for scalable brightness preservation," *IEEE Trans. Consum. Electron.*, vol. 49, no. 4, pp. 1301–1309, Nov. 2003, doi: [10.1109/TCE.2003.1261233](https://doi.org/10.1109/TCE.2003.1261233).
- [34] P. Kandhway and A. K. Bhandari, "An optimal adaptive thresholding based sub-histogram equalization for brightness preserving image contrast enhancement," *Multidimensional Syst. Signal Process.*, vol. 30, no. 4, pp. 1859–1894, Oct. 2019, doi: [10.1007/s11045-019-00633-y](https://doi.org/10.1007/s11045-019-00633-y).
- [35] K. Singh and R. Kapoor, "Image enhancement via median-mean based sub-image-clipped histogram equalization," *Opt. Int. J. Light Electron Opt.*, vol. 125, no. 17, pp. 4646–4651, Sep. 2014, doi: [10.1016/j.ijleo.2014.04.093](https://doi.org/10.1016/j.ijleo.2014.04.093).
- [36] M. V. D. S. T. Gulati, "Histogram equalization for contrast enhancement: A review," *Int. J. Comput. Appl.*, vol. 114, no. 10, pp. 32–36, 2015.
- [37] M. Abdullah-Al-Wadud, M. Kabir, M. A. Dewan, and O. Chae, "A dynamic histogram equalization for image contrast enhancement," *IEEE Trans. Consum. Electron.*, vol. 53, no. 2, pp. 593–600, 2007, doi: [10.1109/TCE.2007.381734](https://doi.org/10.1109/TCE.2007.381734).
- [38] C. Ooi and N. A. M. Isa, "Quadrants dynamic histogram equalization for contrast enhancement," *IEEE Trans. Consum. Electron.*, vol. 56, no. 4, pp. 2552–2559, Nov. 2010, doi: [10.1109/TCE.2010.5681140](https://doi.org/10.1109/TCE.2010.5681140).
- [39] C.-H. Lu, H.-Y. Hsu, and L. Wang, "A new contrast enhancement technique by adaptively increasing the value of histogram," in *Proc. IEEE Int. Workshop Imag. Syst. Techn.*, May 2009, pp. 407–411, doi: [10.1109/IST.2009.5071676](https://doi.org/10.1109/IST.2009.5071676).
- [40] A. S. Parihar and O. P. Verma, "Contrast enhancement using entropy-based dynamic sub-histogram equalisation," *IET Image Process.*, vol. 10, no. 11, pp. 799–808, Nov. 2016, doi: [10.1049/iet-ipr.2016.0242](https://doi.org/10.1049/iet-ipr.2016.0242).
- [41] S. H. Majeed and N. A. M. Isa, "Iterated adaptive entropy-clip limit histogram equalization for poor contrast images," *IEEE Access*, vol. 8, pp. 144218–144245, 2020, doi: [10.1109/ACCESS.2020.3014453](https://doi.org/10.1109/ACCESS.2020.3014453).
- [42] C. Ding, X. Pan, X. Gao, L. Ning, and Z. Wu, "Three adaptive sub-histograms equalization algorithm for maritime image enhancement," *IEEE Access*, vol. 8, pp. 147983–147994, 2020, doi: [10.1109/ACCESS.2020.3015839](https://doi.org/10.1109/ACCESS.2020.3015839).
- [43] Q. Wang and R. K. Tan, "Fast image/video contrast enhancement based on weighted thresholded histogram equalization," *IEEE Trans. Consum. Electron.*, vol. 53, no. 2, pp. 757–764, May 2007, doi: [10.1109/TCE.2007.381756](https://doi.org/10.1109/TCE.2007.381756).
- [44] Y.-R. Lai, P.-C. Tsai, C.-Y. Yao, and S.-J. Ruan, "Improved local histogram equalization with gradient-based weighting process for edge preservation," *Multimedia Tools Appl.*, vol. 76, no. 1, pp. 1585–1613, Jan. 2017, doi: [10.1007/s11042-015-3147-7](https://doi.org/10.1007/s11042-015-3147-7).
- [45] M. Kim and M. Chung, "Recursively separated and weighted histogram equalization for brightness preservation and contrast enhancement," *IEEE Trans. Consum. Electron.*, vol. 54, no. 3, pp. 1389–1397, Aug. 2008, doi: [10.1109/TCE.2008.4637632](https://doi.org/10.1109/TCE.2008.4637632).
- [46] A. K. Bhandari, "A logarithmic law based histogram modification scheme for naturalness image contrast enhancement," *J. Ambient. Intell. Humanized Comput.*, vol. 11, pp. 1605–1622, Feb. 2020, doi: [10.1007/s12652-019-01258-6](https://doi.org/10.1007/s12652-019-01258-6).
- [47] T. L. Kong and N. A. M. Isa, "Bi-histogram modification method for non-uniform illumination and low-contrast images," *Multimedia Tools Appl.*, vol. 77, no. 7, pp. 8955–8978, 2018, doi: [10.1007/s11042-017-4789-4](https://doi.org/10.1007/s11042-017-4789-4).
- [48] S. Mohan and T. R. Mahesh, "Particle swarm optimization based contrast limited enhancement for mammogram images," in *Proc. 7th Int. Conf. Intell. Syst. Control (ISCO)*, Jan. 2013, pp. 384–388, doi: [10.1109/ISCO.2013.6481185](https://doi.org/10.1109/ISCO.2013.6481185).
- [49] P. Babu and V. Rajamani, "Contrast enhancement using real coded genetic algorithm based modified histogram equalization for gray scale images," *Int. J. Imag. Syst. Technol.*, vol. 25, no. 1, pp. 24–32, Mar. 2015, doi: [10.1002/ima.22117](https://doi.org/10.1002/ima.22117).
- [50] K. G. Dhal, M. Sen, and S. Das, "Cuckoo search-based modified bi-histogram equalisation method to enhance the cancerous tissues in mammography images," *Int. J. Med. Eng. Inform.*, vol. 10, no. 2, pp. 164–187, 2018, doi: [10.1504/IJMEL.2018.091209](https://doi.org/10.1504/IJMEL.2018.091209).
- [51] K. G. Dhal, M. Sen, S. Ray, and S. Das, "Multi-thresholded histogram equalization based on parameterless artificial bee colony," in *Incorporating Nature-Inspired Paradigms in Computational Applications*. Hershey, PA, USA: IGI Global, Mar. 2018, pp. 108–126, doi: [10.4018/978-1-5225-5020-4.ch004](https://doi.org/10.4018/978-1-5225-5020-4.ch004).
- [52] K. G. Dhal and S. Das, "Colour retinal images enhancement using modified histogram equalisation methods and firefly algorithm," *Int. J. Biomed. Eng. Technol.*, vol. 28, no. 2, pp. 160–184, 2018, doi: [10.1504/IJBET.2018.094725](https://doi.org/10.1504/IJBET.2018.094725).
- [53] H. Singh, A. Kumar, L. K. Balyan, and G. K. Singh, "Swarm intelligence optimized piecewise gamma corrected histogram equalization for dark image enhancement," *Comput. Elect. Eng.*, vol. 70, pp. 462–475, Aug. 2018, doi: [10.1016/j.compeleceng.2017.06.029](https://doi.org/10.1016/j.compeleceng.2017.06.029).
- [54] M. Wan, G. Gu, W. Qian, K. Ren, Q. Chen, and X. Malague, "Particle swarm optimization-based local entropy weighted histogram equalization for infrared image enhancement," *Inf. Phys. Technol.*, vol. 91, pp. 164–181, Jun. 2018, doi: [10.1016/j.infrared.2018.04.003](https://doi.org/10.1016/j.infrared.2018.04.003).
- [55] P. C. Sen, M. Hajra, and M. Ghosh, *Image Enhancement Using Differential Evolution Based Whale Optimization Algorithm*, vol. 937. Singapore: Springer, 2020.
- [56] A. K. Bhandari, P. Kandhway, and S. Maurya, "Salp swarm algorithm-based optimally weighted histogram framework for image enhancement," *IEEE Trans. Instrum. Meas.*, vol. 69, no. 9, pp. 6807–6815, Sep. 2020, doi: [10.1109/tim.2020.2976279](https://doi.org/10.1109/tim.2020.2976279).
- [57] S. H. Majeed and N. A. M. Isa, "Adaptive entropy index histogram equalization for poor contrast images," *IEEE Access*, vol. 9, pp. 6402–6437, 2021, doi: [10.1109/ACCESS.2020.3048148](https://doi.org/10.1109/ACCESS.2020.3048148).
- [58] E. D. Pisano, S. Zong, B. M. Hemminger, M. DeLuca, R. E. Johnston, K. Müller, M. P. Braeuning, and S. M. Pizer, "Contrast limited adaptive histogram equalization image processing to improve the detection of simulated spiculations in dense mammograms," *J. Digit. Imag.*, vol. 11, no. 4, p. 193, Nov. 1998.

- [59] T. Jintasuttisak and S. Intajag, "Color retinal image enhancement by Rayleigh contrast-limited adaptive histogram equalization," in *Proc. 14th Int. Conf. Control, Autom. Syst. (ICCAS)*, Oct. 2014, pp. 692–697.
- [60] S. Beery, "Pasadena-Houses 2000," California Inst. Technol. Vis., USA, Tech. Rep., 2000. [Online]. Available: http://www.vision.caltech.edu/image_datasets/faces.tar
- [61] S. Beery, "Faces 1999 (Front) database," California Inst. Technol. Vis., USA, Tech. Rep., 1999. [Online]. Available: http://www.vision.caltech.edu/image_datasets/Pasadena-Houses-2000.tar
- [62] S. Bakas *et al.*, "Segmentation labels and radiomic features for the pre-operative scans of the TCGA-GBM collection. The cancer imaging archive," *Natural Sci. Data*, vol. 4, Sep. 2017, Art. no. 170117.
- [63] H. Moradmand, S. Setayeshi, A. R. Karimian, M. Sirous, and M. E. Akbari, "Comparing the performance of image enhancement methods to detect microcalcification clusters in digital mammography," *Iran. J. Cancer Prev.*, vol. 5, no. 2, p. 61, 2012.
- [64] F. Lamberti, B. Montruccio, and A. Sanna, "CMBFHE: A novel contrast enhancement technique based on cascaded multistep binomial filtering histogram equalization," *IEEE Trans. Consum. Electron.*, vol. 52, no. 3, pp. 966–974, Aug. 2006, doi: [10.1109/TCE.2006.1706495](https://doi.org/10.1109/TCE.2006.1706495).



ALI FAWZI was born in Baghdad, Iraq, in 1985. He received the B.Sc. and M.Sc. degrees in computer sciences from Baghdad University, Iraq, in 2006, and 2018 respectively. He is currently pursuing the Ph.D. degree with the School of Computer Sciences, Universiti of Sains Malaysia, Malaysia-Penang. In 2019, he joined the Universiti of Sains Malaysia. From 2008 to 2019, he was at the Iraqi Ministry of Health, Baghdad, where he worked as a Senior Database Designer and an Instructor at the Iraqi Health Information System (HIS). He has some publications related to computer vision and image processing. His current research interests include medical image processing and artificial intelligence.



ANUSHA ACHUTHAN (Member, IEEE) received the Ph.D. degree in computer vision and medical image analysis from Universiti Sains Malaysia, in 2016. She is currently a Senior Lecturer with the Advanced Medical and Dental Institute, Universiti Sains Malaysia. Besides research work, she is also very passionate about online teaching and learning resources. She has developed a MOOC course on scientific writing and delivered workshops on e-learning modules. Her research interests include computational neuroscience, knowledge-guided image analysis, biomarkers analysis for neurological disorders and aging, machine learning, and computer vision. She is a member of ISMRM and IACSIT.



BAHARI BELATON received the B.App.Sc. degree in computer studies from the South Australian Institute of Technology, Australia, the B.Sc. degree (Hons.) from Flinders University, and the Ph.D. degree from the University of Leeds, U.K. He is a Professor with the School of Computer Science, Universiti Sains Malaysia (USM). Currently, he is the Dean with the School of Computer Sciences, USM. His research interests include scientific data visualization, computer graphics, and network security.